

8-2022

The Novel Role Of Dnmbp In Kidney Development

Brandy Walker

Follow this and additional works at: https://digitalcommons.library.tmc.edu/utgsbs_dissertations



Part of the [Cell Biology Commons](#), [Developmental Biology Commons](#), [Medicine and Health Sciences Commons](#), and the [Other Cell and Developmental Biology Commons](#)

Recommended Citation

Walker, Brandy, "The Novel Role Of Dnmbp In Kidney Development" (2022). *Dissertations and Theses (Open Access)*. 1214.

https://digitalcommons.library.tmc.edu/utgsbs_dissertations/1214

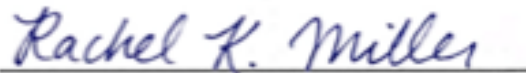
This Thesis (MS) is brought to you for free and open access by the MD Anderson UTHealth Houston Graduate School at DigitalCommons@TMC. It has been accepted for inclusion in Dissertations and Theses (Open Access) by an authorized administrator of DigitalCommons@TMC. For more information, please contact digcommons@library.tmc.edu.

A Novel Role for Dnmbp in Kidney Development

by

Brandy Lynn Walker, B.S.

APPROVED:



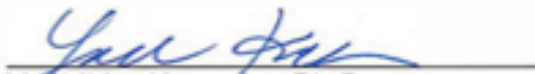
Rachel K. Miller, Ph.D.
Advisory Professor



George Eisenhoffer, Ph.D.



Pierre McCrea, Ph.D.



Yoshihiro Komatsu, Ph.D.



Ruth Heidelberger, MD, Ph.D.

APPROVED:

Dean, The University of Texas
MD Anderson Cancer Center UTHealth Graduate School of Biomedical Sciences

A Novel Role for Dnmbp in Kidney Development

A

Thesis

Presented to the Faculty of

The University of Texas

MD Anderson Cancer Center UTHealth

Graduate School of Biomedical Sciences

in Partial Fulfillment

of the Requirements

for the Degree of

Master of Science

by

Brandy Lynn Walker, B.S.

Houston, Texas

August, 2022

Dedication

This thesis is dedicated to my loving and supportive family.

To my amazing husband who has shown unconditional support throughout this journey, I love you. Without you this would have not been possible.

To my beautiful children, Brandan, Ayden, and Alyssa. Never give up on your dreams because anything is possible when you work hard for it. I love you all so much and know you will do great things in life.

Acknowledgments

I would like to thank my advisor, Dr. Rachel Miller, for being incredibly supportive throughout my MS graduate career. Her support and guidance extended beyond the doors of the lab, and I will forever be grateful for her wisdom and advice, not only in scientific matters, but through personal struggles as well. She was always there to help me see from a different perspective, and even during weeks where every experiment seemed to fail, she would help me see the excitement in what those failures revealed. Rachel, thank you for giving me the confidence to believe in my own ideas, the independence to explore those ideas/experiments, and for always being there when I needed advice or a push in the right direction. You have truly helped me grow not only as a scientist but as a person, and for that I can't thank you enough. I would also like to thank the past and present members of the Miller lab for their contributions and support throughout my thesis research. I want to thank Alexandria (Alex) Blackburn for uncovering my interest in developmental and cell biology with just one talk during the Presidents' Research Award presentation and ultimately leading to my desire to pursue working in the Miller Lab. I want to thank Vanja Krneta-Stankic for always being willing to give me advise or show me new techniques even though she had moved on to her new position as a postdoc in another lab. I especially want to thank Mark Corkins who served as my primary mentor throughout my MS studies and still does to this day even though he has moved on to another lab in another state. Beginning in a new lab, doing unfamiliar research during a pandemic was scary and overwhelming, but Mark made it feel like it was exactly where I was meant to be. His willingness to explain and draw concepts (as many times as I needed) never wavered. He was always there to help me learn new techniques, design new experiments and troubleshoot failed ones, or to just

listen to me vent (a lot) when I was having a bad day and sing random musical showtunes to brighten the mood.

I would like to thank the McCrea lab, Park lab, Malgorzata Kloc, and Adriana Paulucci for all the great feedback and suggestions you gave me during our weekly lab meetings to help me think of new experiments to try, different reagents to use, and develop better ways to present my findings. Additionally, I would like to thank the past and present members of the Komatsu lab. They were always willing to help if there was a reagent we didn't have, if I needed an experimental sounding board, or if I just needed a second set of eyes. I would also like to thank my advisory committee members (Pierre McCrea, George Eisenhoffer, Yoshi Komatsu, and Ruth Heidelberger) for helping me stay on track and always being willing to come together for meetings as often as I wanted. For most students I spoke with, advisory meetings were an inconvenience, something they hated to do and always put off if they could, but for me it was something I looked forward to. The incredible support and encouragement that my committee showed gave me confidence in the work I was doing. I would also like to thank all of the past and present members of the G&E community, as well as the faculty and staff at GSBS.

Most importantly, I would like to thank my parents, family and friends for your encouragement, moral support, and endless understanding throughout this journey. I will be eternally grateful for my all-night study sessions with Sissy, who only *mildly* complained when our subject for the night entailed "gross" biological contents (which was A LOT).

And E.C., I owe everything to you.

A Novel Role for Dnmbp in Kidney Development

Brandy Lynn Walker, B.S.

Advisory Professor: Rachel K. Miller, Ph.D.

Congenital anomalies of the kidney and urinary tract (CAKUT) accounts for nearly one-fourth of all birth defects and more than 40% of pediatric end-stage renal disease, yet only 10-20% of CAKUT cases have a known monogenetic cause. Human kidneys are composed of up to a million epithelial tubules called nephrons. Disruption of nephron development is one of the many congenital anomalies that cause CAKUT, often resulting in chronic or end-stage renal disease which requires transplant. During nephron epithelialization, the formation of stable cadherin-mediated adhesion junctions is essential for maintaining cell-cell contacts. To understand the cell behaviors underlying abnormalities in renal morphology and cyst formation and to facilitate the application of novel treatments for congenital birth defects, a better understanding of the cellular mechanisms driving cell junction formation during nephron formation is needed. Given that adhesion complex components are known to be transported via membrane vesicles, we examine the role of the exocyst-associated scaffolding protein, Dynamin binding protein (Dnmbp), during junction assembly in epithelializing nephric tubules. We show that disruption of Dnmbp affects adhesion and junctional integrity of nephron progenitor cells by significantly reducing junctional E-cadherin localization when compared with standard controls. Additionally, Dnmbp-depleted nephron progenitor cells appear to have disordered membrane borders, further indicating a reduction in junctional integrity. This thesis enhances our understanding of adhesion and junctional integrity of nephron progenitor cells during epithelialization.

Table of Contents

Signature Page	i
Title page	ii
Dedication	iii
Acknowledgments	iv
Abstract	vi
Table of Contents	vii
List of Figures	ix
List of Abbreviations	xi
Chapter 1. Introduction	1
1.1 Kidney Structure and Development	1
1.2 Modeling Nephrogenesis in <i>Xenopus laevis</i>	9
1.2.1 <i>Xenopus</i> Pronephric Development	10
1.3 Cell Interactions	12
1.3.1 Cell Polarity	12
1.3.2 Cell Adhesion	15
1.4 Vesicle Transport.....	17
1.5 Dynamin Binding Protein	18
Chapter Summary	20
Project Aims	21
Chapter 2. Materials and Methods	22
2.1 <i>Xenopus laevis</i> embryos.....	22
2.2 Synthetic mRNA and Morpholinos	22
2.3 Embryo Microinjections.....	23

2.4 <i>Xenopus</i> Whole-Mount Immunofluorescence	23
2.5 Live Imaging of <i>Xenopus</i> Pronephros.....	26
2.6 Image Processing and Statistical Analysis	27
Chapter 3. The role of Dnmbp in nephron epithelialization.	28
3.1 Introduction.....	28
3.2 Dnmbp localization in epithelializing nephric primordium.....	29
3.2.1 <i>Dnmbp</i> localization to cell junctions in epithelializing nephric primordium.....	29
3.2.2 <i>Dnmbp</i> localization relative to vesicles	37
3.3 Dnmbp depletion in developing nephrons.....	39
3.3.1 <i>Dnmbp</i> depletion disrupts <i>E-cadherin</i> localization in developing nephrons.....	39
Chapter 4. Dnmbp in mature <i>Xenopus</i> embryonic kidneys.	45
4.1 Dnmbp localization in relation to mature nephrons.....	45
4.2 Dnmbp depletion in mature <i>Xenopus</i> embryonic kidneys.....	47
4.2.1 <i>Dnmbp</i> depletion disrupts <i>E-cadherin</i> localization in mature <i>Xenopus</i> embryonic kidneys.....	47
Chapter 5. Discussion	50
5.1 Dnmbp-associated vesicle transport affects cadherin-mediated junction formation in epithelializing nephrons.	50
5.2 Future directions.....	53
Chapter 6. Bibliography	55
Vita	72

List of Figures

Figure 1. Anatomy of the Human Kidney	2
Figure 2. Stages of Mammalian Kidney Development	6
Figure 3. Vesicle transport of E-cadherin	17
Figure 4. Diagram of two conserved Dnmbp isoforms	19
Figure 5. Expression of two full-length Dnmbp constructs.	30
Figure 6. Expression of two conserved Dnmbp isoforms results in different subcellular localization patterns in live imaging of Xenopus epidermis	32
Figure 7. Expression of two conserved Dnmbp isoforms in fixed transgenic pax8 reporter Xenopus embryonic kidney cells.	34
Figure 8. In vivo time-lapse imaging of Xenopus windowed kidney.	36
Figure 9. Dnmbp localizes to exocytic vesicles marked by Rab11 in developing Xenopus kidney epithelia.	38
Figure 10. Dnmbp is required for E-cadherin localization to the junctions in epithelializing nephrons.	42
Figure 11. Expression of two conserved Dnmbp isoforms results in different subcellular localization patterns in fixed mature Xenopus embryonic kidney.	46
Figure 12. Depletion of Dnmbp within epithelializing nephric primordium significantly disrupts the localization of junctional E-cadherin within functioning pronephros.	49

List of Tables

Table 1. Major substances reabsorbed and secreted in human nephric regions.	4
Table 2. Table of antibodies and fluorescent probes. Listing of all antibodies and fluorescent probes used for immunostaining.	26
Table 3. Descriptive statistics from ANOVA test of std-control, iControl KD, and Dnmbp KD	44

List of Abbreviations

AJ	Adherens junction
aPKC	atypical protein kinase-C
BAR	BIN/amphiphysin/Rvs
BSA	Bovine serum albumin
CAKUT	Congenital anomalies of the kidney and urinary tract
CAMs	Cell adhesion Molecules
Cdc42	Cell division control protein 42-homolog
CE	Convergent extension
CM	Cap mesenchyme
DFA	Danilchik's for Amy solution
DGO	Diego
DH	Dbl Homology domain
Dnmbp	Dynamin binding protein
DVL	Dishevelled
E-cadherin	Epithelial cadherin
Fmi	Flamingo
FZ	Frizzled
GEF	Guanine Exchange Factor
GFP	Green Fluorescent Protein
hCG	Human chorionic gonadotropin
iControl	Internal control
Ig-CAMs	Immunoglobulin superfamily cell adhesion molecules
MDCK	Madin Darby Canine Kidney

MET	Mesenchymal to epithelial Transition
mGFP	Membrane-tagged-GFP
MOs	Morpholino Oligonucleotides
mRFP	Membrane-tagged-RFP
mRNA	Messenger RNA
NF	Nieuwkoop and Faber
N-WASp	Neural Wiskott-Aldrich syndrome protein
PAR	Partitioning-defective (<i>par</i>) genes
PBS	Phosphate Buffered Saline
PBS-T	Phosphate Buffered Saline containing 0.1% Triton X-100
PBT	Phosphate Buffer containing 2mg/ml BSA and 0.1% Triton X-100
PCP	Planar cell polarity
PIP2	Phosphatidylinositol 4,5-bisphosphate
Pk	Prickle
Rab	Ras-associated binding protein
RFP	Red Fluorescent Protein
SH3	Src Homology-3 domain
Stbm	Strabismus
std-control	Standard control
TCA	Trichloroacetic acid solution
TJ	Tight Junction
UB	Ureteric Bud
VANGL	Van Gough

Chapter 1. Introduction

Kidneys are the quintessential regulators of homeostasis with substantial cellular complexity and functional diversity. They play a fundamental role in blood filtration, nutrient reabsorption, and secretion of unwanted substances [1]. The control of filtrate solute concentration through reabsorption and excretion processes regulates ionic balance, intravascular fluid volume and maintains body fluid osmolarity. The kidneys also produce hormones responsible for various downstream processes such as stimulating production of red blood cells and regulation of blood pressure, in addition to maintaining pH balance and removing drug and metabolic waste products [2].

1.1 Kidney Structure and Development

Structurally, each kidney is divided into three regional areas contained within fibrous tissue called the renal capsule: the cortex, the medulla, and the pelvis (Fig. 1A). The cortex is the outermost region located between the capsule and the medulla. The medulla, which is the innermost region, contains numerous funnel shaped structures known as the renal pyramids. Papillae at the tapered ends of the pyramids merge to form the central region of the kidney known as the renal pelvis, which collects and funnels urine to the ureter [1-2]. Contained within the cortex and medulla are complex microscopic structures called nephrons, the functional units of the kidney (Fig.1B). Adult human kidneys contain approximately one million nephrons which are responsible for filtering the blood to remove waste in the form of urine [1]. Disruption of nephron development is one of the many anomalies that can result in congenital

anomalies of the kidney and urinary tract (CAKUT), which often leads to chronic kidney disease or end-stage renal disease requiring transplant [3-4].

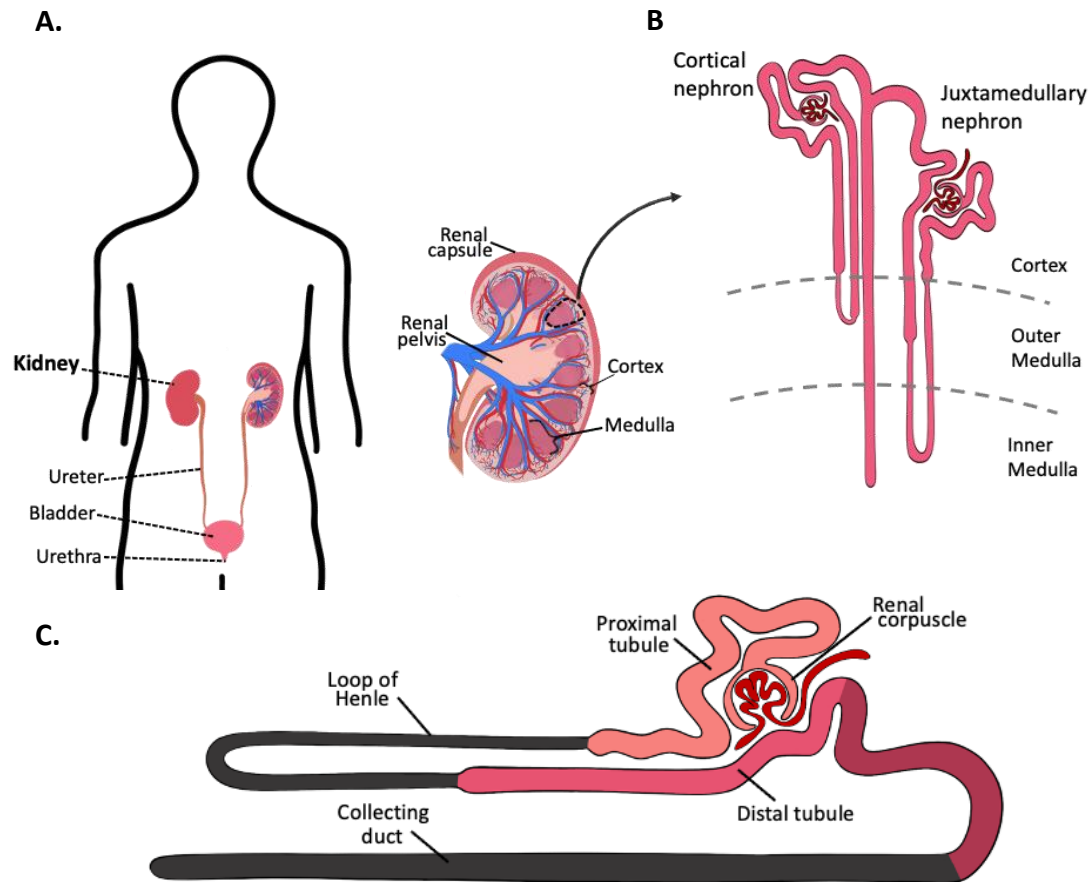


Figure 1. Anatomy of the Human Kidney. Schematic illustrating kidney: (A) anatomical position of the urinary tract (kidneys, ureters, bladder, and urethra) within the body and sagittal kidney section showing regional areas contained within the renal capsule (cortex, medulla, and pelvis) as well as the blood vessels (arteries are red, veins are blue) (B) an expanded wedge of cortex and medulla, illustrating the microscopic nephron position along the corticomedullary axis, and (C) segmentation of a nonintegrated juxtamedullary nephron.

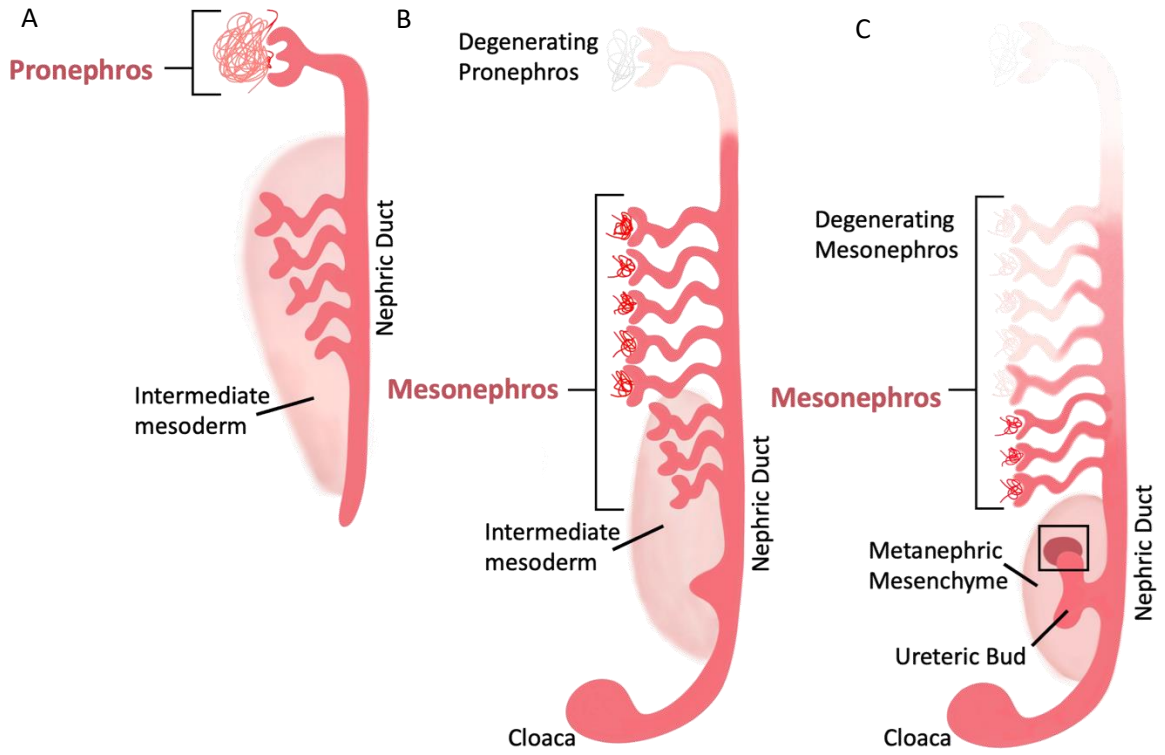
Each nephron (Fig.1C) is composed of five distinct segments: (1) renal corpuscle, (2) proximal convoluted tubule, (3) the loop of Henle, also known as the intermediate tubule (4) distal convoluted tubule, and (5) collecting duct. The renal corpuscle is made up of a complex network of capillaries (glomerulus) encased by a cup-like structure known as the Bowman's capsule. Blood from the afferent arteriole enters the renal corpuscle where it is filtered by the peripheral capillary loops of the glomerulus prior to exiting via the efferent arteriole. The water and solutes removed from the blood due to hydrostatic pressure against the capillary walls enters the Bowman's Capsule becoming primary urine (glomerular filtrate). From the Bowman's capsule, the filtrate enters the renal tubules for further processing through a series of reabsorption and secretion events. These events allow essential nutrients and water to be transported from the renal tubules into the blood via the peritubular capillaries (reabsorption), as well as the movement of unwanted substances from the blood of the peritubular capillaries into the renal tubules (secretion). Each region of the nephron is responsible for the reabsorption and secretion of specific substances (Table 1) through both active and passive transport processes. Following the final processing in the collecting duct, urine moves out of the nephron into the renal pelvis where it exits the kidney to the ureter [2,5-7].

Human Nephron Region	Major Substances Reabsorbed				Substance(s) secreted
Proximal convoluted tubule	Na ⁺ Cl ⁻ K ⁺	H ₂ O	Glucose Amino acids	HCO ₃ ⁻ Ca ⁺² Mg ⁺²	H ⁺ NH ₄ ⁺ Urea Creatinine
Loop of Henle	Na ⁺ Cl ⁻ K ⁺	H ₂ O	HCO ₃ ⁻ Ca ⁺² Mg ⁺²		Urea
Distal convoluted tubule	Na ⁺ Cl ⁻	H ₂ O	Ca ⁺²		(nothing)
Collecting duct	Na ⁺	H ₂ O	HCO ₃ ⁻		H ⁺ K ⁺

Table 1. Major substances reabsorbed and secreted in human nephric regions.

Each nephron region is responsible for reabsorption and secretion of specific substances. The major substances reabsorbed by the human nephron through active and passive transport includes sodium (Na⁺), chloride (Cl⁻), potassium (K⁺), calcium (Ca⁺²), magnesium (Mg⁺²), bicarbonate (HCO₃⁻), and water (H₂O).

Depending on the species, the mature kidney uniquely develops in two or three successive forms, each of which is dependent on the preceding structure (Fig. 2A-C). Renal development occurs in a cranial to caudal fashion starting with the most simplistic form of the kidney called the pronephros, followed by the mesonephros and ending with the final, most complex form, the metanephros. The pronephros is composed of simple tubules that originate from bilateral condensations of the intermediate mesoderm. In mammals, the pronephric kidney is thought to be non-functional; however, it is required for the development of the superseding forms. As the pronephros begins to regress, the mesonephros develops caudally and replaces it, ultimately fusing with the cloaca, and contributing to the formation of the bladder.



D

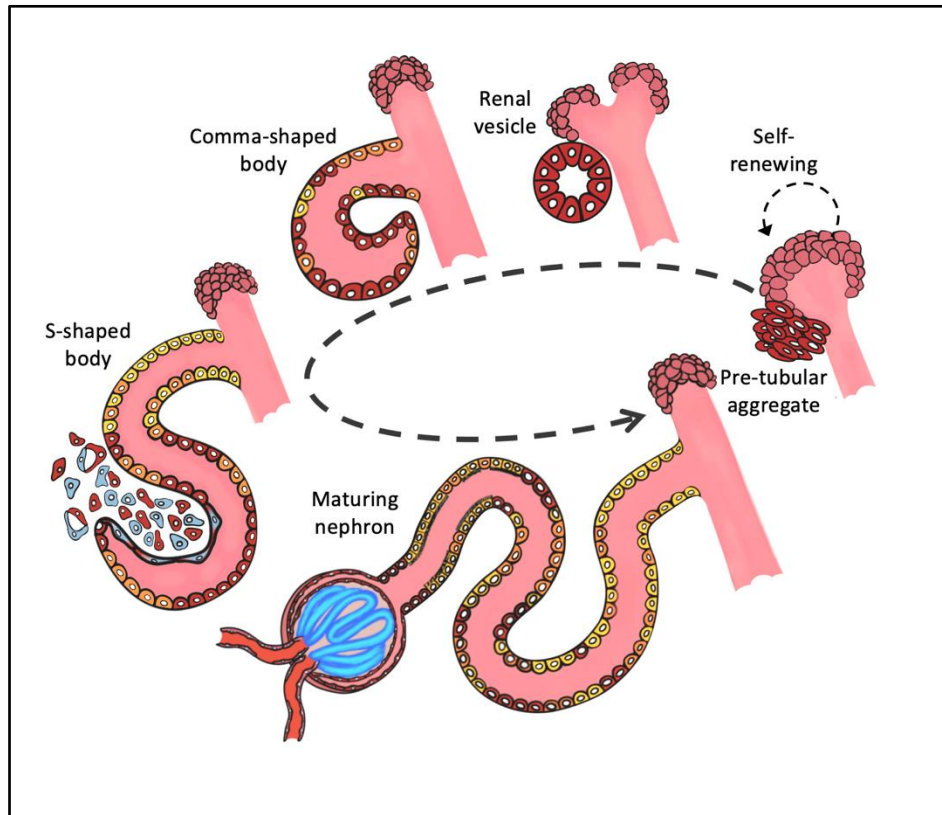


Figure 2. Stages of Mammalian Kidney Development

Mammalian kidneys develop from a region ventral to the anterior somites in a unique process that occurs over distinct, successive stages: The pronephric stage, the mesonephric stage, and finally the metanephric kidney (shown in Fig.1 above), which is the final kidney form in amniotes. (A) The pronephros is the first and most simplistic structure formed and is required for the development of superseding forms. (B) As the pronephros begins to regress, the mesonephros develops posterior to it as the replacement structure, ultimately fusing with the cloaca and contributing to the formation of the bladder. As the mesonephros continues to develop, reciprocal and sequential inductive interactions between the ureteric bud and surrounding mesoderm initiate the early events required for metanephric development. (C) Degeneration of the mesonephric kidney structure begins and early events of metanephric kidney induction proceed. Condensation of metanephric mesenchyme around branching ureteric bud tips form cap mesenchyme (area indicated by small black box). (D) Expanded view of the self-renewing cap mesenchyme, illustrating the sequential events of nephron development.

In amniotes, including reptiles, birds and mammals, the pronephros and mesonephros are transient embryonic organs. However, in vertebrate anamniotes, such as fish and amphibians, the pronephros serves as a functional excretory organ during development and is replaced by the mesonephros as its final form during the juvenile and adult stages [27]. The metanephros is the final and most complex form of the kidney in reptiles, birds, and mammals. It develops from reciprocal and sequential inductive interactions between the ureteric bud and surrounding mesenchyme [8]. The ureteric bud (UB) develops as a dorsal outgrowth from the posterior region of the nephric duct, also known as the Wolffian duct [9]. The newly emerged UB extends into the metanephric mesenchyme where it undergoes a series of dichotomous divisions, ultimately forming the highly branched urinary collecting system of the mature adult kidney. As the metanephric mesenchyme condenses around the tips of the branching ureteric tree, regions known as the cap mesenchyme (CM) form (Fig. 2D). Cap mesenchyme is composed of a multipotent population of nephron progenitor cells [11]. As ureteric branching events occur, a subset of these self-renewing cells separate away from the CM to form pre-tubular aggregate that will eventually become a nephron. The mesenchymal nephric progenitor aggregate cells will undergo a multistep process to transition from a mesenchymal to an epithelial lineage and ultimately form a polarized spherical epithelial structure called the renal vesicle that subsequently fuses with the ureteric duct [16-18]. The mesenchymal to epithelial transition (MET) is identifiable by various cellular changes, including shifts in cell polarity and cadherin-mediated epithelialization, among others [17,30]. As the renal vesicle further develops, a cleft in the vesicle forms to create the comma-shaped

body structure, followed by development of a second cleft to produce the S-shaped body structure and ultimately giving rise to the highly organized epithelial tubules that make up the nephrons responsible for filtering the body's blood to remove waste in the form of urine [16-18].

Kidney organogenesis is a highly conserved process among vertebrates, with many similarities regarding cell types, inductive events, signaling pathways, and nephric segmentation and structure between the vertebrate groups [12-13]. The pronephros originates from bilateral condensates of the intermediate mesoderm in both mammals and amphibians, with similar signaling cascades driving differentiation and morphogenesis [8,12-15]. Although in amniotes the pronephric kidney is transient and likely non-functional embryonic organ, in amphibians such as *Xenopus laevis* (hereafter referred to as *Xenopus*) the pronephric kidney serves as a vital excretory organ during embryogenesis [11].

1.2 Modeling Nephrogenesis in *Xenopus laevis*

Xenopus are freshwater frogs possessing many qualities that make them a useful *in vivo* model to study kidney development and disease. The *Xenopus* embryonic kidney, known as the pronephros, is an easily accessible, simple organ, which shares structural and functional similarities to the mammalian nephron (Fig. 3).

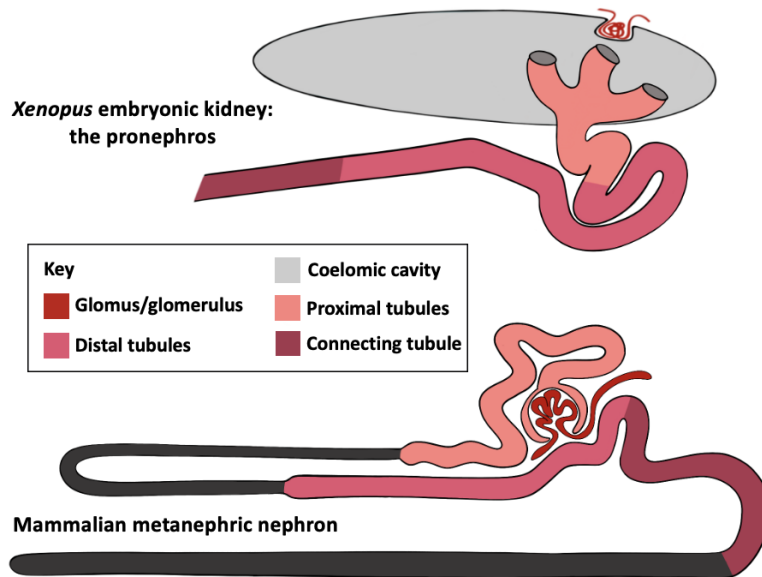


Figure 3. Conserved segmentation pattern of *Xenopus* pronephros and mammalian metanephric nephrons.

As a single, nonintegrated nephron that resides just below a translucent surface ectoderm, the *Xenopus* embryonic kidney offers experimental simplicity in a functionally complex embryonic organ. With a simple hormone injection, *Xenopus* females can be easily induced to ovulate, resulting in three to five clutches of eggs laid the following day. Each clutch typically contains many hundreds of robust eggs (500-1000) that undergo external, synchronized development when fertilized *in vitro*.

The large embryo size, approximately ten times the size of a mouse embryo, and rapid development of *Xenopus* allows for easy experimental manipulation and visualization throughout the entire course of embryogenesis [25-26]. Additionally, the previously established cell-fate map of *Xenopus* early blastula stage embryos enables targeted microinjection into known regions that are fated to become specific structures [19-22] allowing tissue-specific, unilateral genetic manipulation.

1.2.1 *Xenopus* Pronephric Development

Xenopus tadpoles develop functional, bilateral pronephric kidneys in fewer than three days (tadpole stage 38-40) post fertilization, each containing a glomus, tubules, and duct. Analogous to the metanephric glomerulus, the glomus is responsible for vascular filtration; however, organizational differences between the glomerulus and glomus results in blood filtrate deposition site variances. Filtrate from the glomerulus is deposited into the Bowman's capsule and is concentrated directly into the proximal tubules whereas glomus filtrate is deposited into a coelomic cavity and moved into the tubules by ciliary action of nephrostomes. The tubules reabsorb water and nutrients, while the duct excretes waste out of the body via the cloaca [17,23,27]. Pronephric precursor cells are specified from intermediate mesoderm and segregate into nephric components in both mammals and amphibians [16-17]. In the developing *Xenopus* embryo during late gastrula and early neurula stages (stage 12-15), various signals from anterior somites induce intermediate mesodermal precursor cells to the nephric fate, contributing to the renal field. Patterning and subsequent specification of the nephric field defines the morphological segments of the pronephros, which are first evident at early tailbud (stage 25/26) when the nephric mesoderm can be seen as a

distinct, solid mass of cells below the anterior somites. Shortly thereafter, the three ciliated nephrostomes become distinguishable (stage 28), followed by initial formation of a lumen (stage 30) and fully functional pronephros in stage 38-40 tadpoles [17,23,26-29].

Xenopus pronephric development, as well as nephric development in general, is regulated by numerous families of transcription factors and signaling molecules, some of which will be discussed here and others in subsequent sections in this chapter. The spatial and temporal regulation of mesodermal induction [31], early pronephric patterning events [14,16,23,32-33], and subsequent molecular regulation of pronephric differentiation and morphogenesis [34-37] are all critical aspects of pronephros development. In *Xenopus*, the anterior-posterior axis of the nephric primordium is defined by expression of the LIM-type homeodomain transcription factor *lhx1*[38] (formerly *lim1*). In addition, the Pax family transcription factor, *pax8*, is also expressed during the earliest stages of nephric primordium establishment [33] in a distinct, yet overlapping, region and can synergize with *lhx1*, potentially playing a role in spatially restricting *lhx1* expression [32,39]. Mediolateral patterning of the pronephros begins later in the neurula stage to distinguish glomerular primordium from those of the tubules. This process begins when the Wilms' tumor suppressor gene WT1 is expressed in the medial glomerular primordium, resulting in the restriction of *pax8* and *lhx1* to the lateral regions [31]. Dorsoventral patterning of the pronephros occurs at tailbud stages 26-30 when *Wnt4* and members of the Notch pathway are restricted to the dorsal compartment [27].

1.3 Cell Interactions

Cellular interactions mediated by numerous pathways, molecular crosstalk, and direct cell contact sites facilitates and regulates the formation of biological tubules. In addition to the inductive interactions between epithelial ureteric bud cells and the surrounding mesenchymal cells, previously described in section 1.1, the coordinated interactions of signaling and adhesion molecules, various protein complexes, as well as growth and transcription factors are critical to the development and maintenance of the nephron. Proper nephron formation and function depends heavily upon the precise structural organization of nephric epithelial cells, which is determined by the morphological changes that result from processes such as cell polarization, adhesion, signaling, and vesicle transport, among others.

1.3.1 Cell Polarity

The establishment of nephric cell polarity arises from mechanical and biochemical asymmetries along organized 3-dimensional axes within cells, or across the 2-dimensional plane of the tissue. Apical-basal polarity, which is specific to epithelial cells, is formed by asymmetrical distribution of intracellular components within three distinct types of membrane borders of specialized structure and function: the apical (cell-environment interaction) membrane, the basal (cell-matrix interaction) membrane and two lateral (cell-cell interaction) membranes [40]. Segregation of the membrane surfaces arises from coordinated interactions of multiple cellular processes and protein complexes, including polarity-generating signaling networks and polarized vesicular trafficking, among others [41-42]. The Par, Crumbs, and Scribble polarity complexes are key components of apical-basal polarity-generating signaling networks

in epithelial cells [42]. The Par complex, consisting of *Par3*, aPKC, Par6 and Cdc42, and the Crumbs complex, composed of Crb, Pals, and PatJ, define the apical membrane surface. The Scribble complex, which is made up of *Scrib*, Dlg and Lg1, defines the basolateral membrane domain. Intercellular adhesion also facilitates polarity when apical and basolateral regions become separated by the belt-like barrier formed when the cortical actin network becomes tethered to the junctional complexes. Dynein-dependent transport of Par3 along the actin microfilaments is one example of this apical-basal polarity establishment. Clustering of the Par complex components in epithelial cells is dependent on aPKC phosphorylation of Par3, facilitating the apical cortex localization of aPKC-PAR6 and displacement of Par3 due to binding partner competition [43]. Retention of aPKC-Par6 at the apical surface is dependent on active Cdc42-GTP binding to Par6 [40]. Cdc42 bound to annexin upstream at phosphatidylinositol 4,5-bisphosphate (PIP2) rich apical membranes [44] is locally activated by a guanine nucleotide exchange factor protein (GEF) [45].

In addition to apical-basal polarity, epithelialized cells are polarized across the two-dimensional plane of the tissue, a phenomenon known as planar cell polarity (PCP). Planar polarization requires not only the intrinsic polarity of the individual tissue cells, but also the acquired polarity of the collective cell population arising from coordinated intercellular communication [47]. Genetic studies of uniform cell organization in *Drosophila* wing cell hair identified a central set of six cellular factors (referred to as core PCP genes) responsible for the individual, intrinsic polarity of epithelial wing cells, including, Strabismus (Stbm; also known as as Van Gogh; VANGL in vertebrates) [54], Prickle (Pk) [55], Frizzled (Fz; FZD in vertebrates) [51-52], Dishevelled (Dsh; DVL

in vertebrates) [56], Diego (Dgo; ANKRD6 in vertebrates) [57], and Flamingo (Fmi; CELSR in vertebrates) [49,53]. The four-pass transmembrane protein Stbm and the cytosolic protein Pk subcellularly localize to proximal junctions, the seven-pass transmembrane Wnt receptor Fz and the cytosolic proteins Dsh and Dgo localize to distal cell junctions, and Fmi, a seven-pass atypical cadherin, localizes to both the proximal and distal junctions [50]. The subcellular polar distribution of the core PCP components at their respective membrane regions results in the formation of a putative intercellular communication complex, allowing extracellular domains within the membrane interface between cells to receive directional regulatory signals [48]. Directional information is directed by upstream PCP genes and downstream PCP effector genes. When ligands secreted by upstream PCP genes stimulate the extracellular receptor domain, the signal is transmitted into the cell to the cytoplasmic proteins associated with that signaling complex. This leads to activation of the downstream PCP effector gene responsible for initiating the intracellular signaling cascade driving the planar-polarized behavior [58]. The coordinated directional cell movement during biological tube formation is one of many examples of planar-polarized behavior [47-60]. During nephron morphogenesis, convergent extension (CE) movement, facilitated by mediolateral intercalation of multi-cellular rosettes, drives the elongation of *Xenopus* pronephric tubules. Furthermore, when the PCP signaling network is disrupted, not only does nephric tubule elongation fail to occur, but rosette topology and polarized intercalation is disrupted, suggesting non-muscle myosin II may also be affected [59-60]. Other studies have shown non-muscle myosin II cooperates with actin to facilitate adherens junction assembly via E-cadherin

accumulation [62-63], drives cell-cell contact expansion in the presence of RhoA flares [65], and is an essential component in regulating the mechanical forces necessary for coordinated contractile cell movements [63] and junctional reinforcement [64]. Notably, many processes in which are regulated by, or have some influence on, adhesion-mediated cell polarity.

1.3.2 Cell Adhesion

As was previously eluded, cell associations are vitally important to a tissue's morphogenesis, structure, and function, including the epithelial tissue of a nephron. Adhesive contacts are stabilized by the formation of cell junctions, which are composed of large multiprotein complexes. These adhering junctions tether cells to one another, or surrounding environment, act as barriers between cells, or mediate intercellular communication [67]. The molecular architecture and functionality of these intercellular junctions is established by the specificity of the cell adhesion molecules (CAMs) mediating them. Typically, these molecules are transmembrane receptor proteins with extracellular domains for establishing the adhesive contact point, and intracellular domains for cytoplasmic protein interactions, such as actin binding adaptor proteins [67]. In epithelial cells, the formation of cell-cell adhesion junctions, including tight junctions (TJ), adherens junctions (AJ), and desmosomes, are essential for maintaining the integrity and polarity of cells and tissues [66,69-71]. In vertebrates, the most apically located junctional complexes are the TJs [75]. Junctional assembly, stimulated by direct interaction of previously mentioned PCP genes [74], results in a network of "sealing strands" creating an intercellular barrier between the apical (lumen-facing) and lateral (cell-interacting) membrane regions around the

circumference of the entire cell. In mammalian (rat) renal tubules, TJ morphology has been shown to be variable, depending on tubule segment location and transepithelial resistance it is subjected to [72-73]. Cadherin-mediated anchoring junctions, including AJs, provide the physical and mechanical support required for connecting cells within a tissue to one another. Upon first contact between two neighboring epithelial cells, cadherin-mediated AJ assembly is initiated [66,61]. Classical cadherin family adhesion molecules are transmembrane proteins that mediate cell-cell adhesion via calcium-dependent homophilic interaction, joining neighboring cells. Although this homophilic ligation of extracellular domains between cells is required for initiating the cell-cell contact and prompting cytoskeleton rearrangement, it must be strengthened and reinforced to avoid endocytic degradation and maintain the cell-cell contact [63-64,68]. This is facilitated by the cadherin-binding partners p120catenin and β -catenin, as well as other adaptor proteins, resulting in junctional complex attachment to the actin cytoskeleton [64,73]. The recruitment and junctional reinforcement of AJs is perpetual loop of constant recycling. Membrane rearrangements required for the physiological function of a tissue and cellular repair resulting from injury or disease, requires a continual supply of junctional components to be imported, exported, and shuttled around to not only maintain the pivotal, intercellular connections, but also the overall integrity of the tissue.

1.4 Vesicle Transport

It is well established that junctional components are transported to and from the plasma membrane by intracellular vesicles, and membrane turnover plays an essential role in homeostasis and remodeling of dynamic tissues. Membrane associated proteins, such as cadherins, are constantly being internalized with the plasma membrane through endocytosis, sorted and then shuttled back via exocytic vesicles along the actin-myosin cytoskeletal network, if they are not selected for degradation (Fig.3) [77,79] Whether it is newly synthesized E-cadherin moving to its intended position at the plasma membrane or cell surface E-cadherin being internalized and relocated during tissue morphogenesis, remodeling or repair, there is generally always some form of intracellular trafficking machinery involved [64-66,88,96]. Vesicular transport has been shown to impact adherens junction formation and maintenance in a variety of contexts [86-91,95]. The endocytic pathway has been shown to play a central role in the internalization of apical

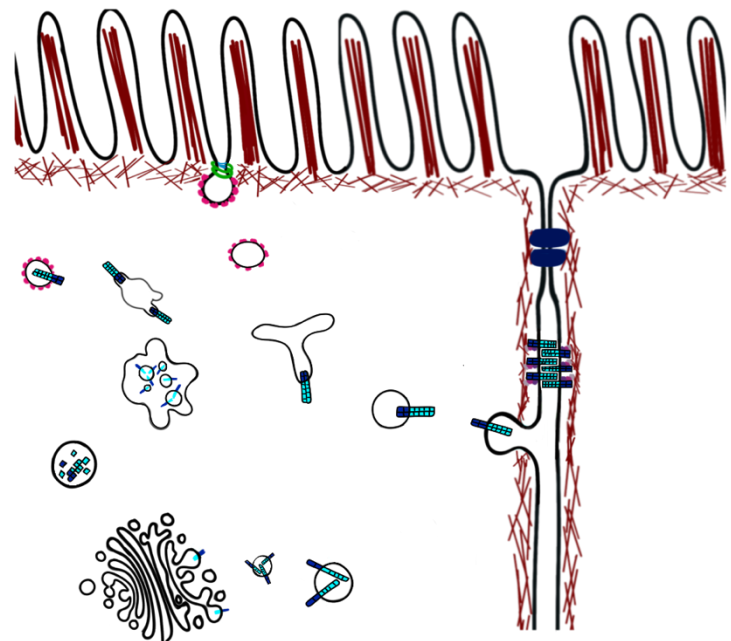


Figure 3. Vesicle transport of E-cadherin

A simplified schematic showing endocytosis of junctional E-cadherin and subsequent salvaging via Rab11-dependent recycling endosome transport back to the plasma membrane.

junction components due to tissue damage and cell migration [79,95]. Dynamin-2, in addition to its known role in endocytic vesicle scission, has been shown to localize to the Golgi complex of epithelial cells, facilitating the release of Clathrin-coated buds for trans Golgi vesicle transport [98]. Transport through the exocytic pathway also plays a critical role in E-cadherin localization to the plasma membrane. Exocytic vesicle regulators and effector proteins, including Rab family GTPases and the Rho family small GTPase Cdc42, as well as several components of the exocyst complex, play a pivotal role in E-cadherin delivery and accumulation to membrane junctions [84,88,94,97-98]. Rab11 regulation of vesicular transport, exocytosis from the trans Golgi network and recycling endosome transport, plays a central role in polarized membrane protein localization and turnover, as well as lumen formation and assembly of primary cilia. Depletion of Rab11 in *Drosophila* epithelial tissues and MDCK cells results in intracellular accumulation of E-cadherin, reduced junctional integrity, and inhibition of cyst formations required for lumenogenesis in MDCK 3D cell cultures [88-89]. Apical membrane docking of the Rab11-dependent transport vesicles is regulated by the Rho family small GTPase Cdc42 when bound to the aPKC/Par3/exocyst complex. However, that target regulation can only occur if Cdc42 is locally activated by the Guanine exchange factor (GEF) known as Dynamin binding protein (Dnmbp) [45].

1.5 Dynamin Binding Protein

Dynamin Binding Protein (Dnmbp) is a multidomain scaffolding protein involved in various cellular processes and regulatory pathways. As a key regulator of the small

GTPase Cdc42, Dnmbp plays an essential role in vesicle transport, the establishment of cell polarity, tissue morphogenesis, and cell-cell junction assembly [44-45,80,84].

The unique domain architecture of Dnmbp consists of four N-terminally located Src Homology-3 (SH3) domains, a centrally located Dbl Homology (DH) domain, and a C-terminally located BIN/amphiphysin/Rvs (BAR) domain that is followed by two additional SH3 domains (Fig.4.) The four N-terminal SH3 domains can independently

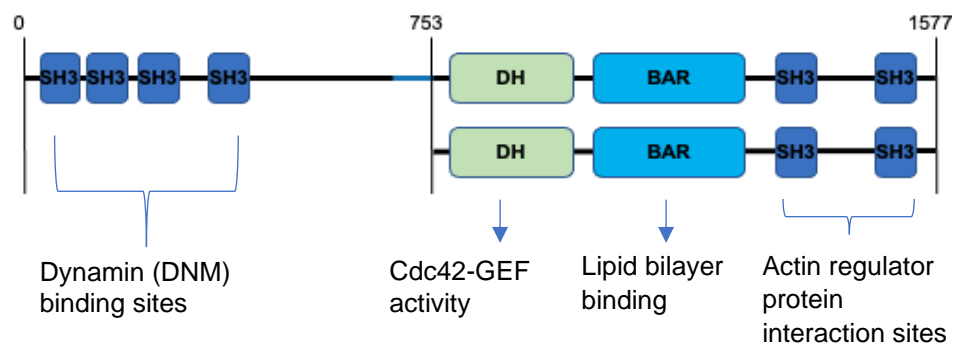


Figure 4. Diagram of two conserved Dnmbp isoforms

Schematic representation of the domain organization of Dnmbp.

SH3 ≡ Src homology-3 domain; DH ≡ Dbl homology domain;

BAR ≡ BIN/amphiphysin/Rvs domain.

bind dynamin, which is known for its role in lipid bilayer bending and scission during endocytosis [98] as well as stimulate N-WASP-dependent actin assembly via its C-terminal SH3 domain [106], resulting in a functional scaffold between endocytic and actin regulatory pathways [98]. In addition to the N-terminal binding capability of Dnmbp directly to dynamin, the C-terminal BAR domain of Dnmbp could also provide aid in dynamin scission as it has its own membrane bending capabilities [100].

However, the N-terminal SH3 domains upstream of the Rho GTPase binding DH domain result in autoinhibition, blocking Cdc42 binding and activation, as well as membrane binding capability of the BAR domain [100]. Prior studies, conducted in HEK293 cells have shown that the tricellular tight-junction-associated protein component tricellulin (a member of the Marvel protein family) releases the N-terminal SH3 intramolecular inhibition when the N-terminal domain of tricellulin binds to the SH3-C2 (SH3 number six) domain of Dnmbp [49]. An alternate method proposed to facilitate release of the autoinhibiting N-terminal SH3 domain, speculates that protein truncation and/or post translational modifications, including phosphorylation, could be a mechanism for removing the N-terminal regulator of DH containing proteins [100]. Nevertheless, interaction between Dnmbp and Cdc42 continue to occur resulting in the regulation of Cdc-42 GTPase activation. Previous work has shown that Dnmbp influences ciliary assembly and tubulogenesis through activation of Cdc42 [80,44,84], as well as being required for facilitating proper spindle orientation [95] and junctional configuration in epithelial tissues [78]. Additionally, published work in *Xenopus* (frog) has revealed that Dnmbp is essential for *Xenopus* embryonic kidney development [97].

Chapter Summary

Dnmbp is a Cdc42-specific guanine nucleotide exchange factor (GEF) associated with exocytic vesical trafficking that is required for nephrogenesis. However, the mechanisms by which Dnmbp is influencing nephron development have yet to be elucidated. Given that Dnmbp is associated with vesicle trafficking in other contexts, and the well-established knowledge that junctional components are

transported via secretory vesicles, our goal is to use kidney-targeted loss of function and over expression assays to evaluate the integrity of adhesion complexes within the entire kidney, as well as within the nephric epithelia specifically. By elucidating the mechanisms by which Dnmbp perturbs the junctions of epithelializing nephron progenitor cells, we hope to gain a better understanding of developmental abnormalities in tubule morphology and cyst formation. *Thus, the goal of this research study is to determine whether Dnmbp regulates the formation of stable, apical cell junctions during nephron epithelialization.*

Project Aims

Given that Dnmbp is associated with vesicle trafficking in other contexts, and the well-established knowledge that junctional components are transported via secretory vesicles, our working hypothesis is that Dnmbp-associated vesicle trafficking facilitates assembly of cadherin-mediated junctions in epithelializing nephric tubules. Using loss of function approaches in combination with confocal, super-resolution and time-lapse imaging of living and fixed *Xenopus* embryonic kidneys, we will assess the integrity of adhesion complexes within the nephric epithelia of the kidney. **Completion of this aim will determine whether Dnmbp affects adhesion and junctional integrity of nephron progenitor cells during epithelialization.**

Chapter 2. Materials and Methods

2.1 *Xenopus laevis* embryos

Xenopus laevis adult frogs were purchased from Nasco (LM00531MX and LM00713M) and maintained according to standard procedures. Eggs were manually collected from adult pigmented *Xenopus laevis* frogs approximately 14-20 hours post ovulation induction with human chorionic gonadotropin (hCG) injection. Collected eggs were fertilized *in vitro* using macerated sperm and placed in 0.3x MMR. Blastula orientation and stages were determined according to established methods [76] and reared as previously described [25]. All work was conducted in accordance with the University of Texas Health Science Center at Houston, Institutional Animal Care and Use Committee (IACUC) approved protocol #AWC-19-0081.

2.2 Synthetic mRNA and Morpholinos

For mRNA injections, capped mRNA transcripts were synthesized from DNA-plasmids under standard protocols using an SP6 mMessage mMachine transcription kit (ThermoFisher, AM1340M) and purification. pCS2-membrane-tagged-RFP (mRFP) [107], pCS2- membrane-tagged-EGFP (mEGFP) [99], pCS2-Rab-11:GFP [101], and pCS2-*β-galactosidase* [108,109] constructs were gifts from Dr. Raymond Keller's lab, Dr. John Wallingford's lab, Dr. Sergei Sokol's lab, and Dr. Peirre McCrea's lab respectively. pCS2-Dnmbp_GFP and pCS2-ΔN-cDnmbp-GFP constructs were generated using pcDNA3-HA-Tuba (Addgene plasmid 22214) to clone Dnmbp (also known asTuba) cDNA into BcuI/XbaI digested pCS2-GFP vector (cloning done by Epoch Life Science). Additionally, pCS2-Dnmbp_RFP and pCS2-ΔN-cDnmbp-RFP

constructs were also obtained from Epoch Life Science. Formerly developed translation-blocking morpholino Dnmbp MO1 (5'-TCGAACCACCGATCCCACCTCCATC-3') [97] and standard control MO (5'CCTCTTACCTCAGTTACAATTTATA 3') were purchased from GeneTools, LLC (Philomath, OR, USA).

2.3 Embryo Microinjections

Xenopus laevis embryos were microinjected with 10 nL of injection mixture (described below) at the single-cell stage for Western blot analysis, or into the V2 blastomere at the eight-cell stage for embryonic kidney targeted microinjections [22,76,102]. Injection solutions contained synthetic mRNAs alone, or in combination with antisense morpholino oligonucleotides (MOs). Single cell embryos were injected with 20 ng MO for Western blot analysis and 8-cell embryos were injected with 10 ng MO for phenotypic analysis. Concentrations of mRNAs co-injected with MOs, or injected alone, were as follows unless otherwise stated within context: mGFP [0.5ng], mRFP [0.5ng], Dnmbp-GFP or -RFP [1ng], Δ N-cDnmbp-GFP or -RFP [1ng], E-cadherin-GFP [250pg], Rab11-GFP [1ng], β -galactosidase [250pg].

2.4 *Xenopus* Whole-Mount Immunofluorescence

Xenopus laevis embryos underwent kidney targeted microinjections at the 8-cell stage as previously described [22] and were reared to tadpole stage 30-33 [76]. Embryos expressing fluorescent tracer were fixed with MEMFA (3.7% formaldehyde, 4mM MOPS, 2mM EGTA, and 1mM MgSO₄, pH 7.4) for one hour at room temperature or overnight at 4°C. Following fixation, embryos were washed with 100% methanol

(MeOH) twice over ten minutes and rehydrated through a series of phosphate buffered saline (PBS) containing 0.1% Triton X-100 (PBS-T) washes over one hour. Rehydrated embryos were incubated overnight in 20% goat serum diluted in PBS-T at 4°C to prevent non-specific targeting of primary antibody. For detection of Rab11, embryos were fixed with 2% trichloroacetic acid solution (TCA) for 30 minutes at room temperature and washed in 0.3% Triton X-100 diluted in PBS over 30 minutes [96] prior to blocking as described above. Blocked embryos were incubated at 4°C overnight in 10% goat serum with primary antibodies. The following day, primary antibodies were recollected, and embryos were subjected to a series of 1X PBS-T washes for removal of excess antibodies. Primary antibody detection was achieved using fluorophore-tagged secondary antibodies against the host species for each primary antibody (A full list of antibodies and fluorescent probes can be found in Table 2 below). Secondary antibody incubation in 10% goat serum took place at 4°C overnight. The following day, embryos were subjected to a series of 1X PBS-T washes to remove excess antibodies and dehydrated in 100% methanol, before being optically cleared with BABB/Murray's clearing medium (1:2 volume of benzyl alcohol to benzyl benzonate) for confocal imaging. Embryos were identified for proper kidney-targeted injection prior to fixation and/or post staining using an Olympus SZX16 fluorescent stereomicroscope and kidney images were taken using a Zeiss LSM800 confocal microscope.

Primary Antibody	Species	Conc.	Clonal Type	Source
anti-GFP	chicken	1:250	Polyclonal	Abcam cat# ab13970
anti-RFP	rabbit	1:250	Polyclonal	MBL International cat# PM005
anti-GFP	rabbit	1:250	Polyclonal	ICL Lab cat# RGFP-45A
anti-Lhx1	rabbit	1:250	Polyclonal	gift from Dr. Masonori Taira (Taira et al., 1992)
anti-E-cadherin	mouse	1:100	Monoclonal	BD Transduction Laboratories cat# 610182
3G8 antibody	mouse	1:30	Monoclonal	European <i>Xenopus</i> Resource Centre, Portsmouth, UK cat# 3G8.2C11
4A6 antibody	mouse	1:5	Monoclonal	European <i>Xenopus</i> Resource Centre, Portsmouth, UK cat# 4A6.2C10
Secondary Antibody	Target Species	Conc.	Clonal Type	Source
Alexa 488	anti-rabbit	1:500	Polyclonal	Invitrogen cat# A-11008
Alexa 555	anti-rabbit	1:500	Polyclonal	Invitrogen cat# A-21244
Alexa 647	anti-rabbit	1:500	Polyclonal	Invitrogen cat# A-21244
Alexa 488	anti-mouse	1:500	Polyclonal	Invitrogen cat# A-11001
Alexa 555	anti-mouse	1:500	Polyclonal	Invitrogen cat# A-21422
Alexa 647	anti-mouse	1:500	Polyclonal	Invitrogen cat# A-21235
Alexa 488	anti-mouse	1:200	Polyclonal	Jackson ImmunoResearch cat# 715-545-150

Fluorescent Probes	Conc.	Source
FITC-conjugated lectin from <i>Erythrina cristagalli</i>	1:500	Vector labs, FL cat# 1141
Phalloidin-Alexa 568	1:40 1:200	Invitrogen cat# A12380
Phalloidin-ifluor 488	1:200	Abcam cat# ab176753
diamidino-2-phenylindole (DAPI)	1:500 1:1000	Thermo Scientific cat# 62247

Table 2. Table of antibodies and fluorescent probes. Listing of all antibodies and fluorescent probes used for immunostaining.

2.5 Live Imaging of *Xenopus* Pronephros

Xenopus 8-cell stage embryos were microinjected with synthetic mRNA(s) into the V2 blastomere for kidney targeted injection, as described above. Embryos were reared to stage 28-32 [76] and selected for positive kidney injection under a fluorescent stereomicroscope. To obtain high-resolution imaging of the nephric primordium *in vivo*, kidney-windowed embryos were created, as previously described by [103]. Removal of the surface epithelium to expose the developing nephron was accomplished using sharpened forceps (Fisher, NC9404145) under an Olympus SZX16 fluorescent stereomicroscope. Microsurgical procedures were performed in plastic petri dishes coated with 2% agar containing Danilchik's for Amy (DFA) solution (53 mM NaCl, 5 mM Na₂CO₃, 4.5 mM Potassium Gluconate, 32 mM Sodium Gluconate, 1 mM CaCl₂, 1 mM MgSO₄, buffered to pH 8.3 with 1 M bicine) supplemented with 1 g/L of Antibiotic Antimycotic solution (1:100, Sigma, A5955). Live images were acquired using a Zeiss LSM800 microscope with Airyscan detector.

2.6 Image Processing and Statistical Analysis

E-cadherin localization between nephron progenitor cell junctions was detected by whole-mount fluorescence immunostaining and confocal microscopy. Junctional integrity was quantified by measuring the fluorescence intensity of E-cadherin along individual cell-cell borders using the Zen Lite image processing software and profiling tool. Analysis of E-cadherin intensity within the Dnmbp-KD kidney compared to the std-control kidney was conducted using Prism software.

Chapter 3. The role of Dnmbp in nephron epithelialization.

3.1 Introduction

The viability and integrity of all tissues within multicellular organisms is critically dependent upon the interconnection of the cells that form them. These cells not only have to establish and maintain a physical connection, but they also must remain in constant communication to coordinate and facilitate each tissue's physiological function. Within the kidneys, cells must establish contacts to generate the epithelial tubules that make up the nephrons. During nephron epithelialization, the formation of stable cadherin-mediated adherens junctions is essential for establishing and maintaining cell-cell contacts and cytoskeletal intercellular connections, as well as facilitating polarized cellular rearrangements and intracellular molecular transport. Gene expression studies have demonstrated the presence of Dnmbp in the developing *Xenopus* pronephric kidney [97]. Previous work in MDCK cell cultures has also shown that Dnmbp influences ciliary assembly and tubulogenesis through activation of Cdc42 [80,44,84], a small GTPase known to associate with components of the exocyst complex [92,93]. Disruption of Cdc42, which is activated via its interaction with the DH domain of Dnmbp, results in ciliary defects and cyst formation within the kidney [84]. Additionally, published work from the Miller lab has revealed that Dnmbp is essential for *Xenopus* embryonic kidney development and depletion of Dnmbp results in the disruption of nephrogenesis [97]. However, the mechanisms by which Dnmbp is influencing nephron development have yet to be elucidated.

The viability and integrity of all tissues within multicellular organisms is critically dependent upon the interconnection of the cells forming it. These cells not only have

to establish and maintain a physical connection, but they also must remain in constant communication to coordinate and facilitate the tissue's physiological function. During nephron epithelialization, the formation of stable cadherin-mediated adhesion junctions is essential for establishing and maintaining cell-cell contacts and cytoskeletal intercellular connections, as well as facilitating polarized cellular rearrangements and intracellular molecular transport. Gene expression studies have demonstrated the presence of Dnmbp in the developing *Xenopus* pronephric kidney [97]. Previous work in MDCK cell cultures has also shown that Dnmbp influences ciliary assembly and tubulogenesis through activation of Cdc42 [80,44,84], a small GTPase known to associate with components of the exocyst complex [92,93]. Disruption of Cdc42, which is activated via interaction with the DH domain of Dnmbp, results in ciliary defects and cyst formation within the kidney [84]. Additionally, published work from the Miller lab has revealed that Dnmbp is essential for *Xenopus* embryonic kidney development and depletion of Dnmbp results in the disruption of nephrogenesis [97]. However, the mechanisms by which Dnmbp is influencing nephron development have yet to be elucidated.

3.2 Dnmbp localization in epithelializing nephric primordium

3.2.1 Dnmbp localization to cell junctions in epithelializing nephric primordium

Based on our labs previously published data indicating Dnmbp is required for nephrogenesis [97], and the knowledge that mesenchymal progenitor cells must establish stable cell-cell contacts to form nephric epithelia, we hypothesized that Dnmbp would localize to apical cell junctions during nephron epithelialization. Whole-

mount immunofluorescent analysis in combination with confocal, super-resolution and time-lapse imaging of live and fixed *Xenopus* embryonic kidneys (stage ~30) were utilized to assess the subcellular localization of Dnmbp with specific interest in cell junctions.

Although overexpression of Dnmbp in the *Xenopus* pronephric kidney has been shown to result in cilia and tubulogenesis disturbances [97], our goal was to utilize the overexpression to provide insight

into the different mechanisms employed by two of the naturally occurring Dnmbp isoforms. Thus, as a first step to gain a clearer understanding of the role Dnmbp has during nephron epithelialization and to visualize subcellular

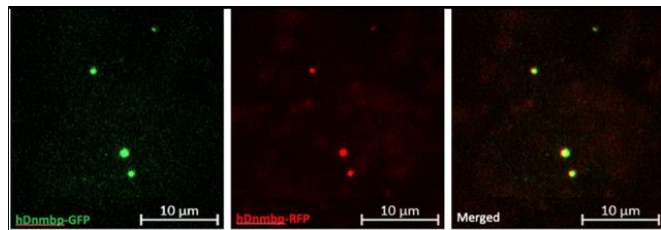


Figure 5. Expression of two full-length Dnmbp constructs. Dnmbp-GFP (green) colocalizes with Dnmbp-RFP (red) in *Xenopus laevis* epithelia. Scale bars measure 10 µm.

localization of Dnmbp *in vivo*, GFP and RFP labeled constructs of two naturally occurring human Dnmbp splice isoforms (full-length Dnmbp isoform a and Dnmbp isoform c) were employed. mRNAs for both the human full-length isoform-a (Dnmbp-GFP and Dnmbp-RFP) and short isoform c, which lacks the four N-terminal SH3 domains (Δ N-cDnmbp-GFP and Δ N-cDnmbp-RFP) were microinjected into *Xenopus* embryos. Interchangeable use of the two identical mRNAs containing different fluorescent tags was verified by evaluating their colocalization in *Xenopus* stage 18 embryos prior to experimental use (Fig.5).

To determine whether the constructs could be used in *Xenopus* embryos at dosages in which they could be visualized *in vivo* for live localization assays, single-cell embryos were microinjected with either full length Dnmbp-GFP mRNA or Δ N-cDnmbp-GFP mRNA. Interestingly, upon live imaging of the epidermis, across several different developmental time periods, the two Dnmbp constructs appeared to have strikingly distinct localization patterns (Fig.5). The full-length Dnmbp localized predominantly to puncta within the cells which are likely vesicles (Fig.5A), whereas Δ N-cDnmbp localized predominantly to cell membranes and throughout the cytoplasm. It is also worth noting that (in the observed *Xenopus* epidermis of this study) the junctional expression of Δ N-cDnmbp seemed to decrease overtime as the epithelial cells reached their more mature cuboidal shape. In the neurula stages 18-20 (Fig.6B, left), Δ N-cDnmbp appears heavily concentrated at the cell-cell membranes; however, as development continues (Fig.6B, across panels left to right) it begins to reflect a more diffuse pattern, with slightly higher intensities observed closer in proximity to established or potential tricellular junctions.

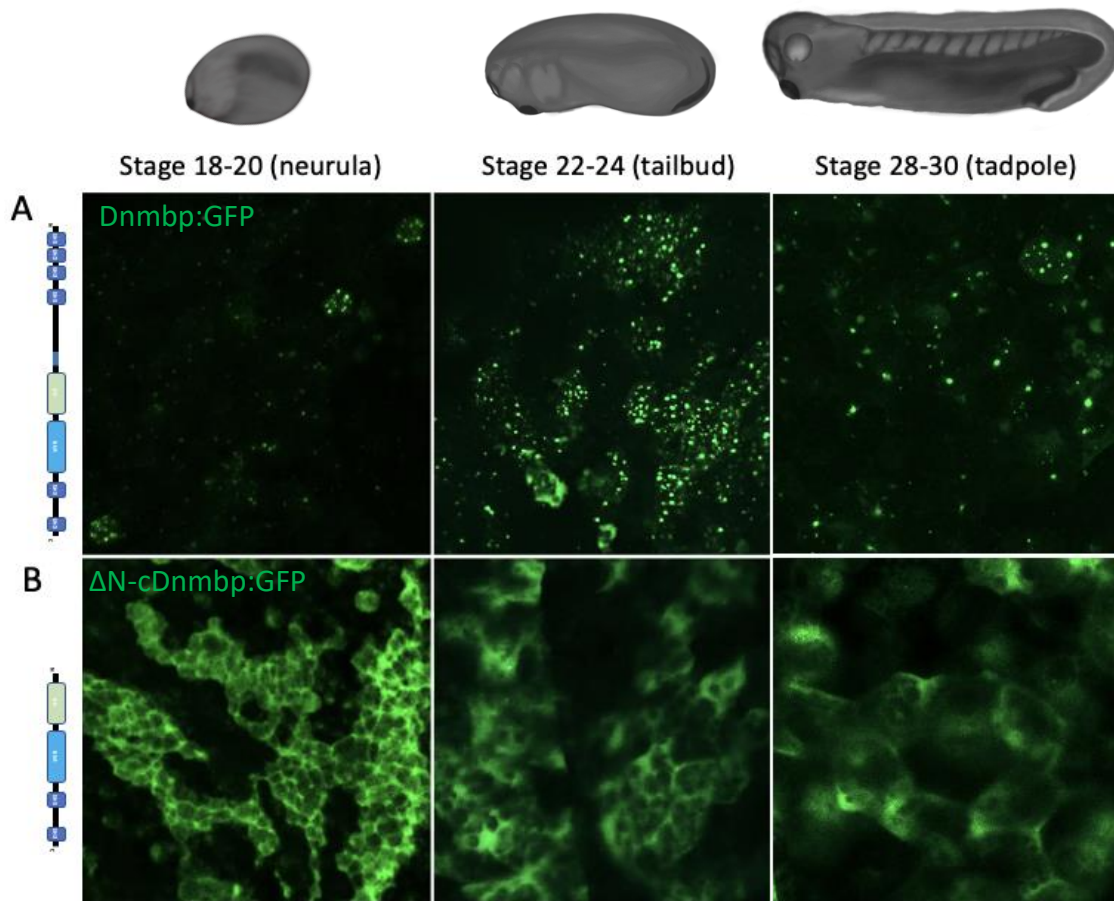


Figure 6. Expression of two conserved Dnmbp isoforms results in different subcellular localization patterns in live imaging of *Xenopus* epidermis
 Strikingly different localization patterns were observed between (A) the full length Dnmbp-GFP construct localization and (B) the Δ N-cDnmbp-GFP construct lacking the N-terminal SH3 domains

Because Dnmbp has been shown to directly interact with junctional components and attenuate apical-basal polarity in various epithelial cell culture lines [49,104], as well as exert influences over several key developmental processes in the kidney [44,80,84-85,92-93], we decided to further evaluate expression of the constructs within epithelializing nephrons, specifically. Using a transgenic *Xla.Tg(pax8:GFP)* *Xenopus* kidney reporter line, subcellular localization of each construct was evaluated in fixed stage 28 embryonic kidneys. Consistent with the prior observations seen in the epidermis, full-length Dnmbp (Fig.7A) localized in scattered puncta throughout the cell, whereas Δ N-cDnmbp was highly cytoplasmic (Fig.7B). At this stage, in these embryos, defined nephric cell-cell junction membranes were not yet strongly evident; however, a few (presumably newly forming) cell-cell borders with minimal intensities were noted.

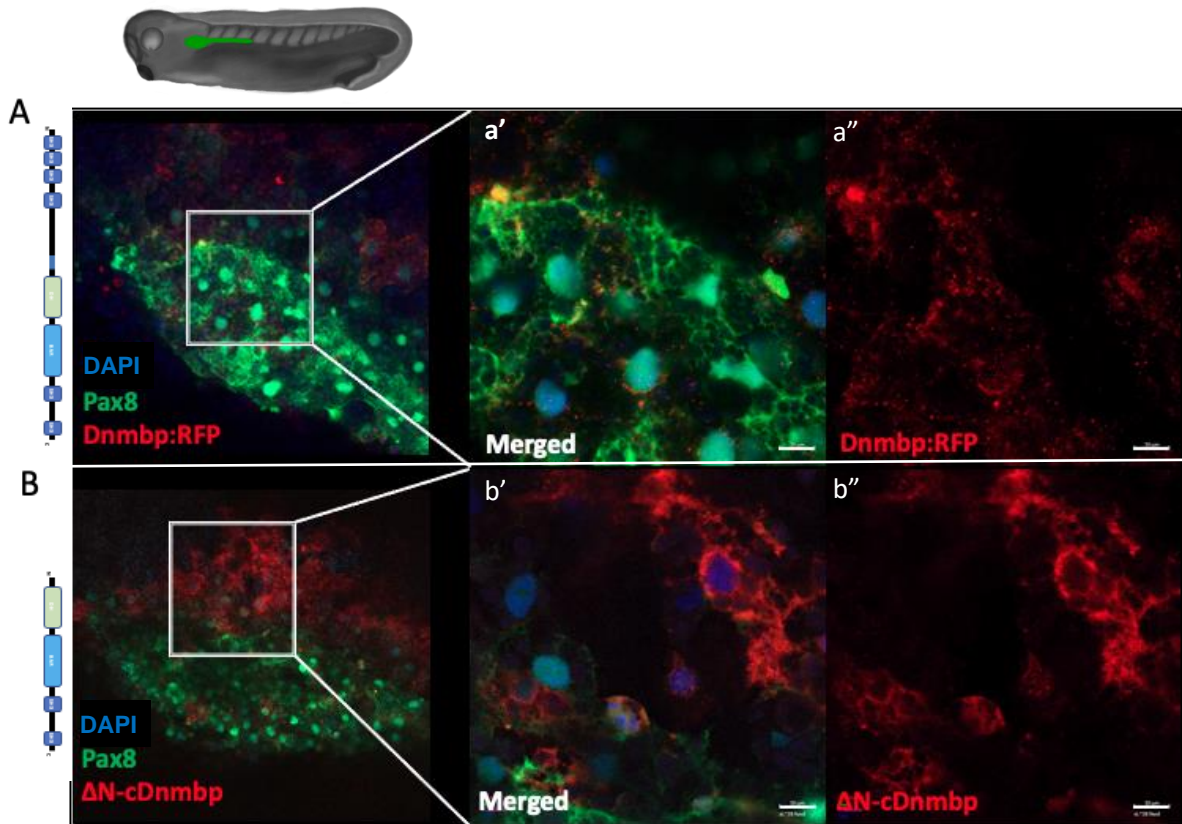


Figure 7. Expression of two conserved Dnmbp isoforms in fixed transgenic *pax8* reporter *Xenopus* embryonic kidney cells. Confocal maximum image projections of whole-mount immunostaining *Xenopus* nephron progenitor cells, marked by transgenic *pax8* reporter expression. Top panel (A) Full length **Dnmbp-RFP** construct localization within nephric primordium; Bottom panel (B) **ΔN-cDnmbp-RFP** lacking N-terminal SH3 domains within nephric primordium; a'-a'' and b'-b'' shows close-up views of white boxes.

The formation of junctions is a dynamic process, with many components moving, changing, and being shuttled around, allowing the collective parts of the system to act as a whole. Therefore, we wanted to see if what appeared to be just scattered puncta throughout the cell were in reality Dnmbp interacting with, or localizing to, the cell-cell contacts in a time and space in which we were just not seeing in the static state being observed. Although the *Xenopus* developing nephron is located just below the surface ectoderm, kidney-windowed embryos, as previously described [105] allowed visualization of this dynamic process without obscurities from the opaque embryonic yoke.

To determine whether the observed scattered puncta of Dnmbp localize to junctions, four-cell embryos were co-injected with mRNAs for the full-length Dnmbp-RFP and a GFP tagged E-cadherin (pCS2-Ecad-GFP) construct. Embryos were first observed under a high-resolution confocal microscope at early tadpole stage ~28 (the time in which epithelialization is beginning); however, the intensity levels for the GFP tag were minimal (data not shown). Therefore, the embryos were left to continue developing and observed again at a time when epithelialization had well been underway. When re-evaluated at stage 34/36, dynamic interactions between the scattered puncta of exogenous full-length Dnmbp was observed closely associating with the tag-GFP at cell-cell contacts. (Fig. 8). In addition to strong presence at cell membrane contacts, E-cadherin-GFP was localized around vesicle-like structures aggregating to what are presumed to be adhering bicellular, tricellular and rosette-like cell junctions. Dnmbp-RFP expression was visible in association with, or in close

proximity to majority of the circular structures, including several instances in which Dnmbp fluorescent expression could be seen filling the E-cadherin sphere.

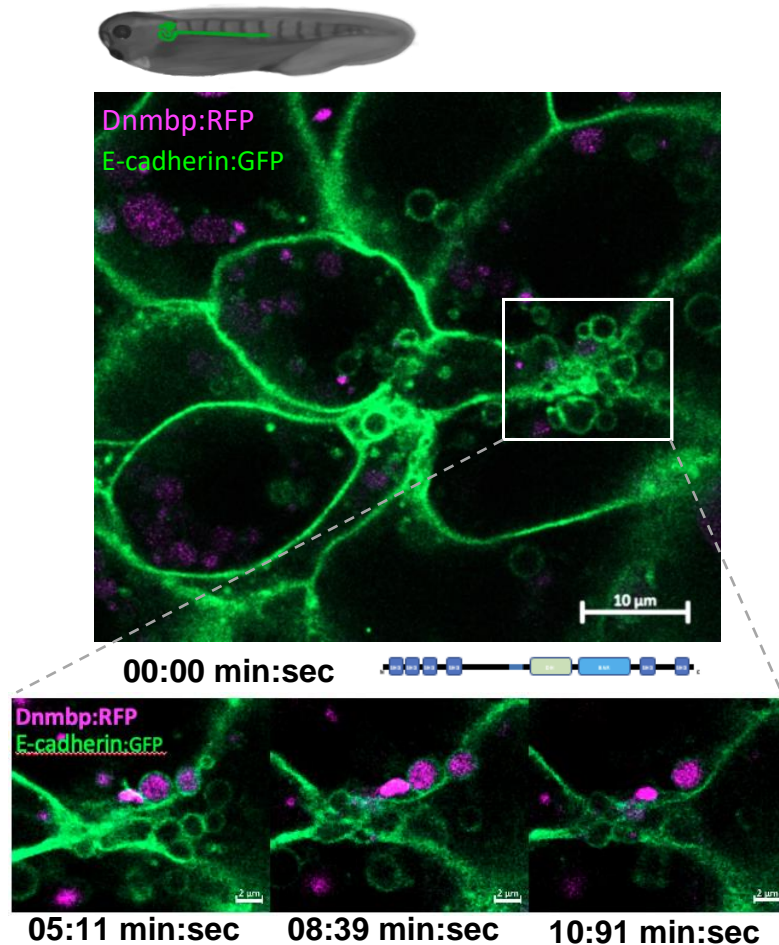


Figure 8. *In vivo* time-lapse imaging of *Xenopus* windowed kidney. Live super-resolution time-lapse imaging shows **Dnmbp (magenta)** and **E-cadherin (green)** constructs localizing in close associations at cell-cell junctions in epithelializing nephric primordium. Bottom three panels represent close-up images of the white box in the top panel at the indicated times below.

3.2.2 Dnmbp localization relative to vesicles

To determine whether the scattered puncta of full-length Dnmbp, observed in prior experiments, is subcellularly localized to vesicles as we hypothesize, the established exocytic vesical marker, Rab11-eGFP construct, was utilized in combination with our Dnmbp-GFP construct, to label exocytic vesicles and evaluate Dnmbp subcellular localization during nephron epithelialization. *Xenopus* 4-cell stage embryos were co-injected into the V2 blastomere with full-length Dnmbp-RFP mRNA and Rab11-eGFP mRNA to assess Dnmbp localization relative to vesicles within epithelializing nephric primordia. High-resolution confocal imaging showed Dnmbp-RFP colocalizing with Rab11-eGFP in stage 30/32 *Xenopus* embryos during epithelialization of the pronephros (Fig.9).

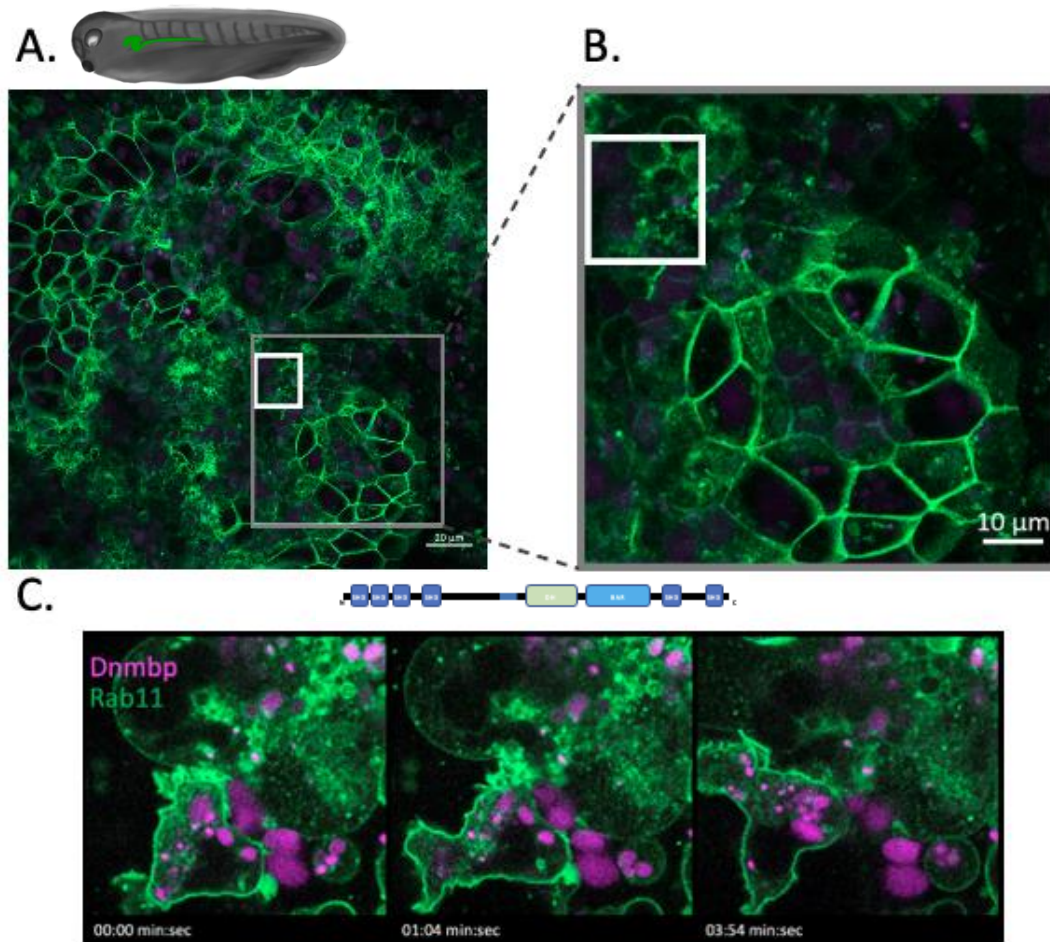


Figure 9. Dnmbp localizes near exocytic vesicles marked by Rab11 in developing *Xenopus* kidney epithelia. Overexpression of **Dnmbp-RFP** (magenta) and **Rab11-GFP** (green) indicate association of Dnmbp and Rab11. A-B. Scale bars measure 10 μm . C. Scale bars measure 5 μm .

3.3 Dnmbp depletion in developing nephrons

Xenopus 8-cell stage embryos were microinjected into the V2 blastomere region for unilateral genetic manipulation of presumptive nephron progenitors [19-22]. A prepared mixture containing either a Dnmbp-specific translation-blocking MO (Dnmbp-KD) and membrane RFP mRNA (mRFP) tracer or a standard control MO (std-Control) and mRFP was used to target presumptive nephron progenitors specifically on one side of the embryo, leaving an internal control (iControl) on the opposing side. All samples received equal volumes and concentrations of treatment injection, and embryos were selected for proper injection target location through microscopic evaluation of mRNA tracer. Stage 30-33 embryos were fixed and subjected to whole-mount immunostaining as described in section 2.4 using primary antibodies against RFP to confirm the presence of co-injected membrane-RFP tracer, as well as antibodies against Lhx1 for early nephron progenitor labeling, and against E-cadherin to assess developing junctions. Additionally, DAPI stain was utilized as a global nuclear marker. Junctional integrity was quantified by fluorescent intensity profiling of E-cadherin along cell-cell borders between mRFP labeled progenitors. Analysis of E-cadherin intensity within the sample treatment conditions was conducted using Prism software.

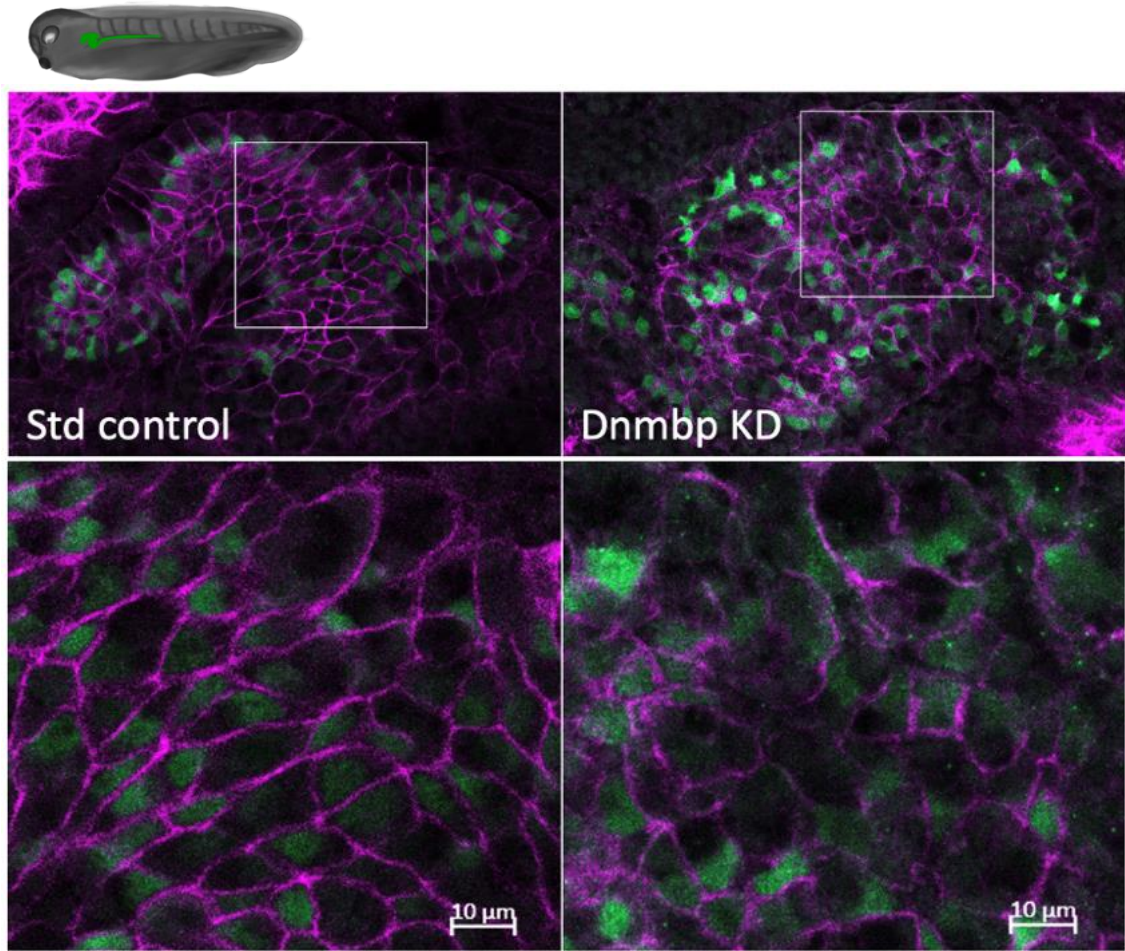
3.3.1 Dnmbp depletion disrupts E-cadherin localization in developing nephrons

To assess the influence of Dnmbp on adherens junction formation during nephron epithelialization, E-cadherin localization at cell-cell junctions was observed upon Dnmbp morpholino-mediated inhibition. Prediction of the effect that Dnmbp-

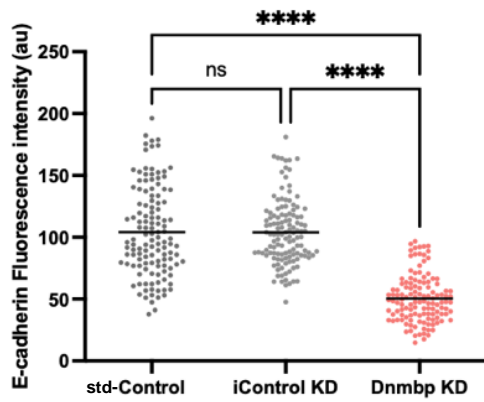
depletion exudes upon junctional integrity took several points into consideration: 1. MO-mediated inhibition within the target tissue often results in mosaic knockdown. 2. Dnmbp-MO1 only blocks translation of the full-length Dnmbp (isoform-a) protein, not the shorter (isoform-c) protein lacking the N-terminal SH3 domains, which has a different 5'UTR. Meaning, not all endogenously expressed Dnmbp in the targeted nephric primordium was depleted.

The data collected over four independent trials shows that E-cadherin fails to localize to the membranes in epithelializing nephrons of *Xenopus* tadpoles upon Dnmbp depletion (Fig. 10.A). Acquired fluorescence imaging suggests lateral diffusion (data not shown) and reduced localization of E-cadherin to the cell - cell membranes of Dnmbp knockdown samples, as well as undulating and/or broken membrane borders. The intensity of E-cadherin is quantitated below (Fig. 10.B). Additionally, preliminary data from Western blot analysis indicate the total E-cadherin concentration in Dnmbp-depleted samples is not reduced (Fig. 10.C).

A.



B.



C.

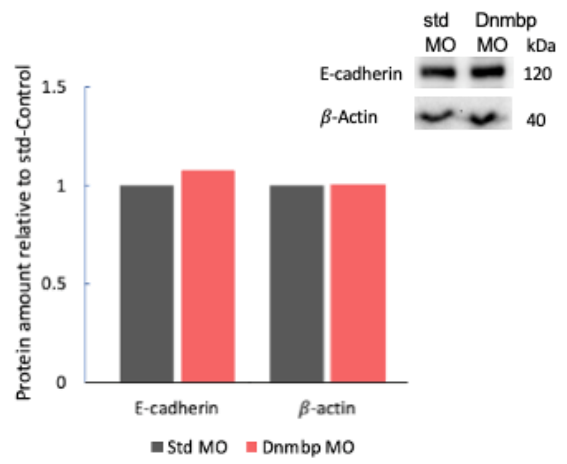


Figure 10. Dnmbp is required for E-cadherin localization to the junctions in epithelializing nephrons.

A. Maximum projection confocal images of E-cadherin (magenta) expression (top) within epithelializing nephric primordium (marked by Lhx1 antibodies (green)) in std-Control and Dnmbp KD embryos (confocal image of iControl KD not shown). Bottom panels represent white box regions of interest. Scale bars measure 10 μm .

B. Scatterplot showing the relative distribution of E-cadherin fluorescence intensity in nephron progenitors of std-control, iControl KD and Dnmbp KD embryos. $N_{\text{std-Control}}=126$ junctions over 4 trials, $N_{\text{iControlKD}}=126$ junctions over 4 trials, and $N_{\text{Dnmbp KD}}=126$ junctions over 4 trials. **** $P < 0.0001$ analyzed by one-way ANOVA.

C. Western blot and corresponding graph of densitometry for E-cadherin and β -actin (control) protein levels for std-Control (Std MO) and Dnmbp KD (Dnmbp MO) injected embryos.

A one-way ANOVA on E-cadherin fluorescence intensity by injection condition (std-Control MO, iControl KD, and Dnmbp KD MO) was conducted under the assumption of X^2 distribution with the null hypothesis that there was no difference in junctional integrity (measured by fluorescence intensity of E-cadherin) among the three groups ($H_1=0$), i.e., $\mu_A = \mu_B = \mu_C$. However, an alternative hypothesis that a 50% reduction of E-cadherin ($H_a = -0.5$) would be sufficient to show an effect from Dnmbp knockdown compared to either control. For example, if the mean intensity of the control is 100, the expected Dnmbp KD mean to show an effect from the depletion would need to be ≤ 50 .

The ANOVA statistical analysis indicated a mean value of $\mu_A = 104.1$ for the std-Control samples, $\mu_B = 103.9$ for the iControl KD samples, and $\mu_C = 50.41$ for the Dnmbp KD samples. The std-Control sample standard deviation was calculated to be $\sigma_A = 35.85$, the iControl standard deviation was $\sigma_B = 26.28$, and the Dnmbp KD standard deviation was $\sigma_C = 19.10$. More descriptive statistics including minimum, maximum, and median values for the three groups are summarized in table 3 and a scatterplot of the relative distributions is shown in figure 10.B (above). Under a predetermined 5% significance level, the ANOVA rejected the null hypothesis given F-statistics = 22.48 and p-value < 0.0001. Follow-up tests using *Tukey HSD* showed that std-Control vs Dnmbp KD was significantly below the threshold with an adjusted p-value of $P < 0.0001$, as was the iControl KD vs Dnmbp KD with an adjusted p-value of $P < 0.0001$. However, when comparing the two control samples (std-Control vs iControl KD) the adjusted p-value was calculated at $P = 0.9970$ and did not fall below the dictated threshold. Therefore, we conclude that among std-Control, iControl KD,

and Dnmbp KD sample groups, at least one group has a different mean fluorescence intensity of E-cadherin, and there is not sufficient evidence to reject the alternative hypothesis.

Descriptive Statistics				
Group	Minimum	Median	Maximum	Mean (Std. Deviation)
std-Control (A)	37.71	96.80	196.3	104.1 (35.85)
iControl KD (B)	47.52	102.3	181.1	103.9 (26.28)
Dnmbp KD (C)	14.68	47.73	96.79	50.41 (19.10)

Table 3. Descriptive statistics from ANOVA test of std-control, iControl KD, and Dnmbp KD

Chapter 4. Dnmbp in mature *Xenopus* embryonic kidneys.

4.1 Dnmbp localization in relation to mature nephrons

Dnmbp localization in mature embryonic kidneys was assessed by injecting 1ng of either full length GFP-tagged Dnmbp mRNA or the short isoform GFP-tagged Dnmbp (pCS2-hDnmbp_truncation-GFP) mRNA into the V2 blastomere of 8-cell stage *Xenopus* embryos. Subcellular localization of the GFP-tagged constructs was detected by whole-mount immunofluorescent staining of stage 40 embryos fixed in methanol-free fixative prior to staining with antibodies against GFP to visualize Dnmbp, against β -catenin, a structural component fundamental to cadherin-based adherens junctions, as well as antibodies against 3G8 and 4A6 to label mature nephrons and phalloidin staining to visualize F-actin.

Upon imaging the mature nephron at tadpole stage ~40, the full-length Dnmbp construct appeared to have strikingly different localization patterns compared to the construct lacking the N-terminal SH3 domains (Fig. 11).

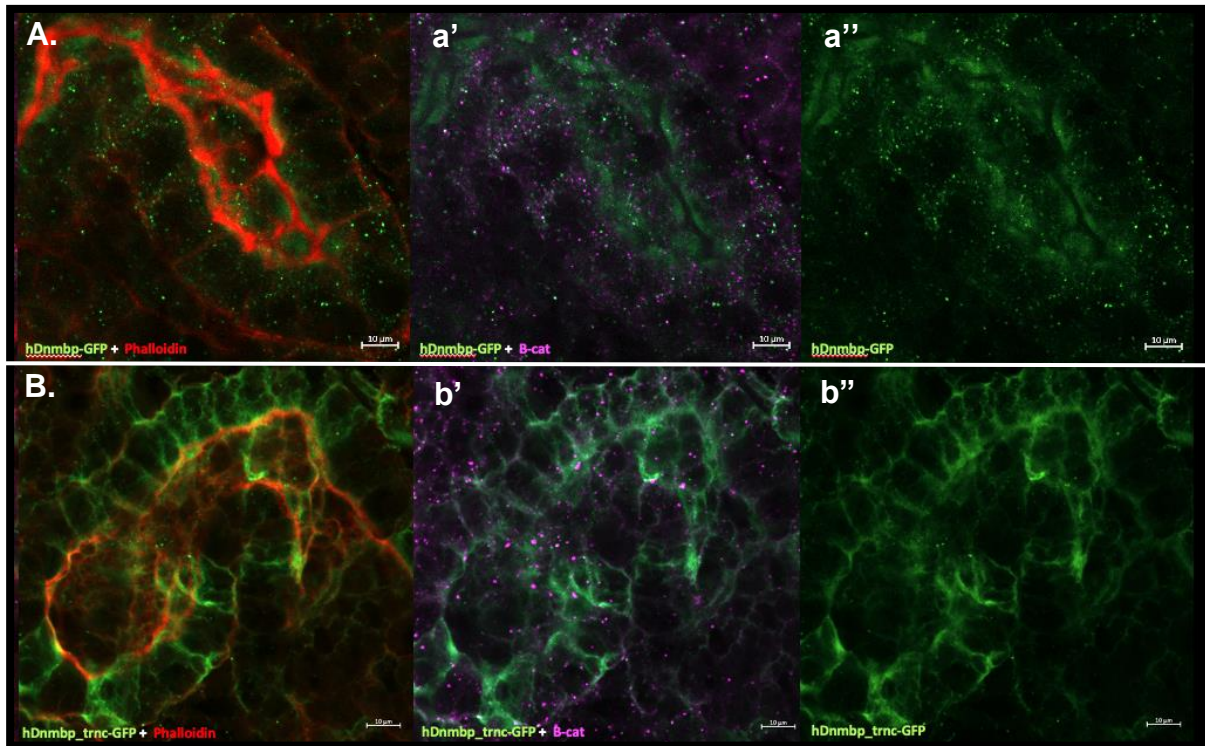


Figure 11. Expression of two conserved Dnmbp isoforms results in different subcellular localization patterns in fixed mature *Xenopus* embryonic kidney.

Overexpression of Dnmbp constructs results in strikingly different localization patterns in mature tadpole stage 40 embryonic kidney (A) the full length **Dnmbp-GFP** construct localization appears concentrated just below the apical surface and scattered punctate regions within the cells. (B) the **ΔN-cDnmbp-GFP** construct lacking the N-terminal SH3 domains localizes predominately to cell borders and in the cytoplasm. Embryos were co-stained with **Phalloidin (red)** for visualization of F-actin as well as **β-catenin (magenta)**.

4.2 Dnmbp depletion in mature *Xenopus* embryonic kidneys

4.2.1 Dnmbp depletion disrupts E-cadherin localization in mature *Xenopus* embryonic kidneys

E-cadherin localization to mature-nephron cell junctions was detected by whole-mount immunofluorescence staining and confocal microscopy. Stage 40-42 embryos were fixed by formalin prior to immunostaining with primary antibodies against RFP to confirm the presence of co-injected membrane-RFP tracer and against E-cadherin to assess junction integrity. FITC-conjugated lectin was used for mature nephron labeling, as well as DAPI staining to label nuclei. Quantification of junctional integrity was achieved by measuring the fluorescent intensity of E-cadherin along individual pronephric cell-cell borders with confirmed mRFP presence. Analysis of E-cadherin intensity within the Dnmbp-KD kidney compared to the un-injected internal control kidney (iControl) and std-Control kidney was conducted using Prism software. Significant data indicated that depletion of Dnmbp within the mature *Xenopus* embryonic nephron disrupts the localization of junctional E-cadherin (Fig. 12). There was no significant difference found between the Std-control and iControl of the KD embryos. To address whether un-injected cells adjacent to injected cells have E-cadherin defects, fluorescent intensity profiling of E-cadherin along individual cell-cell borders when only one cell had mRFP expression present (DnmbpKD+RFP), as well as fluorescent intensity profiling of junctional E-cadherin along cell-cell contacts when neither cell had mRFP expression present (DnmbpKD-RFP). In addition, fluorescent intensity profiling of junctional E-cadherin in mature nephron cells of the iControl

kidney (image not shown). Analysis of E-cadherin intensity within the Dnmbp-KD kidney compared to the std-Control kidney was conducted using Prism software. The mean fluorescence intensities used for analysis of iControl cell junctions was acquired from the same embryos in which the injected side data was collected, and the same number of junctions were profiled for each side within each embryo in the trial. Data analysis indicates that E-cadherin localization to the junctions is significantly disrupted in the Dnmbp depleted mature nephron, even when mRFP tracer is not present in the junctions of injected kidney nephron progenitor cells (Fig. 12). The data also indicate that junctional E-cadherin localization of iControl kidneys is not significantly affected by Dnmbp depletion treatments on the other side of the embryo.

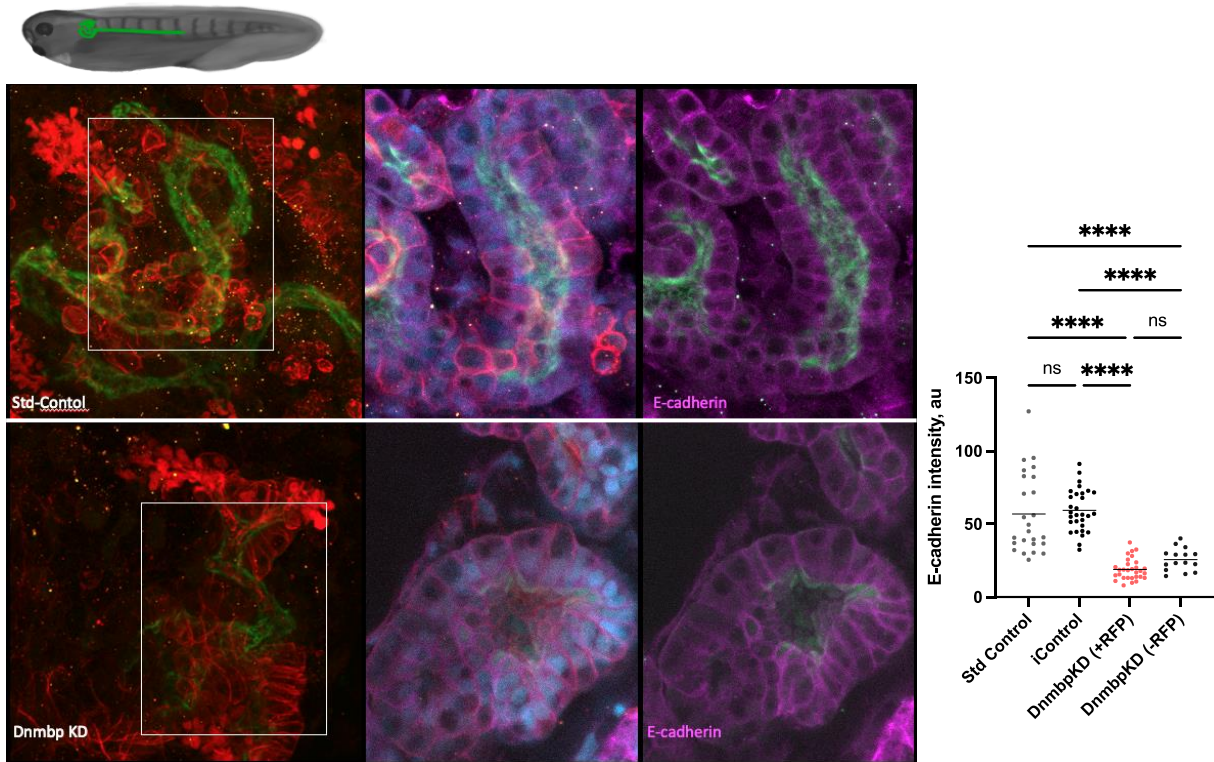


Figure 12. Depletion of Dnmbp within nephric primordium significantly reduces the localization of junctional E-cadherin within mature pronephros.

Depletion of Dnmbp within epithelializing nephric primordium disrupts the localization of junctional E-cadherin (magenta) to mature nephrons labelled with lectin and DAPI. mRFP co-injected with Dnmbp-MO as tracer. Analysis compares E-cadherin intensity quantitated in cells identified with mRFP tracer for Std-control, iControl (uninjected side of KD embryo) and Dnmbp-KD (+RFP). Cells not showing mRFP tracer within the Dnmbp-KD [Dnmbp-KD (-RFP)] kidneys identified by mRFP tracer were also quantified to determine if all cells within the KD kidney are receiving morpholino-mediated depletion.

Chapter 5. Discussion

5.1 Dnmbp-associated vesicle transport affects cadherin-mediated junction formation in epithelializing nephrons.

Using *Xenopus* embryonic kidneys as a model system, we show that Dnmbp facilitates cadherin-mediated cell junction assembly during nephron epithelialization by regulating transportation of apical junction complex components. Ultimately, this affects the integrity of cell-cell junctions and morphology of the nephric epithelium (Figure 13).

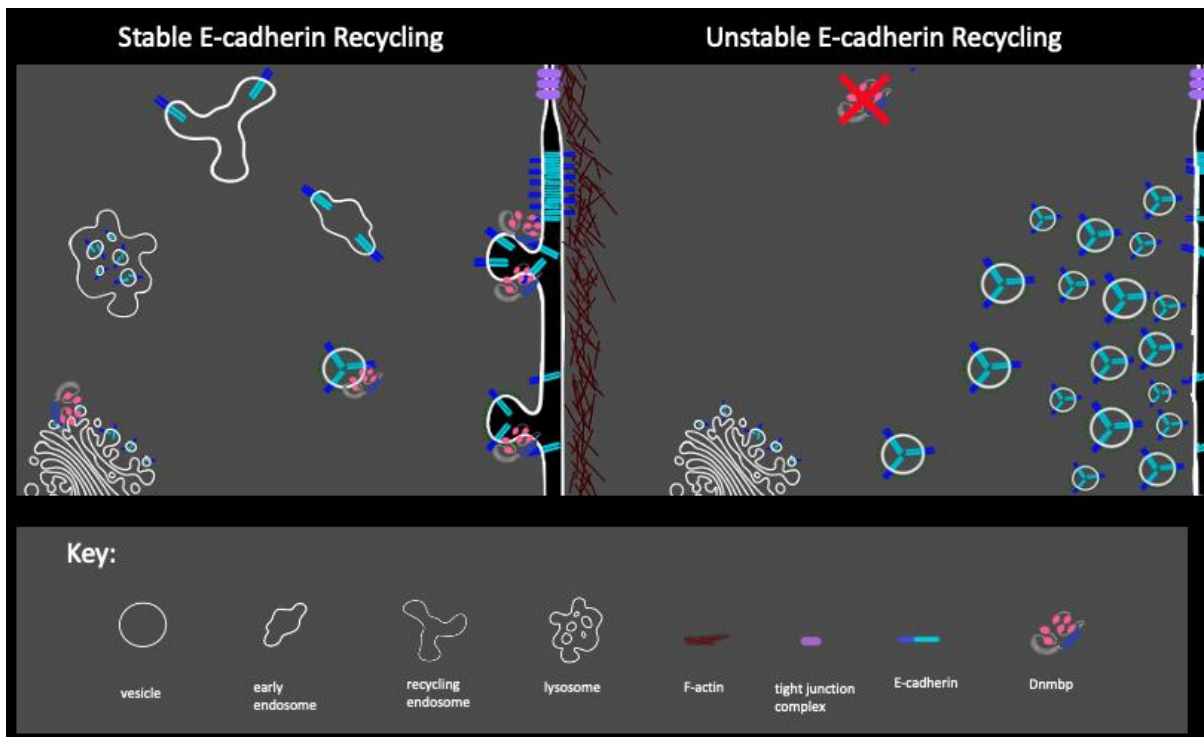


Figure 13. Summary of Chapter 5 findings.

These findings have several important implications for the regulation of cell contact formation during nephric epithelialization.

Here we show that Dnmbp localizes to cell borders and puncta within the cytoplasm of epithelializing nephric primordium and is required for E-cadherin association at cell-cell contact sites. Exogenous expression of two naturally occurring DNMBP splice isoforms reveals distinctly different subcellular localization patterns in the developing pronephric kidney. Previous work in cell culture has implicated Dnmbp membrane localization is associated with apical junction complex components and influences junctional configuration by local regulation of Cdc42 [78], and it has been speculated in the past that Dnmbp activity is regulated by autoinhibition between the N-terminal SH3 domain(s) and C-terminal SH3 domain(s) [49]. It was also shown that proline rich peptide binding of the C-terminal Dnmbp SH3 domains (whether intramolecular or intermolecular is still unknown) was needed to facilitate a conformational change in structure of Dnmbp to release the binding inhibition [49]. By releasing this autoinhibition the binding interaction sites of the DH and BAR domains become accessible, making Dnmbp activation of downstream effector genes that utilize these sites possible. Seeing as the BAR domain of Dnmbp is required for its direct interaction with lipid bilayers [100], it makes sense that the full-length protein would have a more difficult time localizing to the plasma membrane. As the Δ N-cDnmbp (Fig.6B) construct has no N-terminal SH3 domains to compete for C-terminal SH3 binding, the protein is left in a perpetual “on” state. Thus, it would be easy to see how this could give Δ N-cDnmbp a higher binding affinity for the plasma membrane and/or intracellular membranous network, without the inconvenience of waiting on competing up-stream genes to bind the C-terminal before lipid binding regions or downstream effector binding sites are exposed.

Upon morpholino mediated depletion of Dnmbp, E-cadherin localization to the cell membranes was disrupted but preliminary data from Western blot analysis suggests there is no change in total E-cadherin protein abundance, further indicating the disruption of E-cadherin at the membrane is due to a failure of E-cadherin transport mechanisms (Fig.10). The observed lateral diffusion of E-cadherin upon Dnmbp depletion suggest a scenario in which the recycling of E-cadherin from the lateral membrane could be impaired. Prior work in MDCK cells has indicated that Dnmbp can regulate Rab11 transport vesicle docking ability at the plasma membrane [44-45], supporting our E-cadherin recycling impairment hypothesis. However, our findings of reduced junctional E-cadherin are a contradiction of prior Dnmbp-depletion studies in cell culture, which found that Dnmbp knockdown did not alter the concentration of E-cadherin at the cell-cell junctions but did increase the apical surface area [78]. This could possibly be a consequence of junctional profiling only accounting for the E-cadherin accumulated at the apical cell borders and not the molecules distributed to the lower lateral portions of the junction contributing to the increase in junctional surface area. This distortion of junctional geometric structure was however in agreement with our findings of undulated cell-cell membranes and increased lateral diffusion upon immunostaining of E-cadherin in Dnmbp-depleted embryos.

Nevertheless, constant internalization of membrane components is essential to the integrity of cell borders, and protein sorting and recycling is pivotal to that process. Our preliminary data demonstrating Dnmbp associates with E-cadherin at the membranes and localizes near Rab11 marked vesicles supports recent findings that Rab11-dependent vesicles require Dnmbp activation of Cdc42 for recycling

endosome transport back to the plasma membrane [44-45]. Interestingly, the data also showed Dnmbp clusters within the lumen of large Rab11-GFP vesicles that remained stationary throughout the course of live imaging. Similar accumulated vesicles were described previously in a study that showed Rab11 initiates endosomal maturation by binding the coiled coil domain of a negative regulator of endosome maturation and then translocating from the recycling endosome to autophagosomes [103]. Taking this under consideration with our observations of stagnant vesicle movement, it would be possible to imagine a role for Dnmbp in the endocytic pathway that is independent of vesicle scission or Cdc42 activation for membrane docking. These observations could suggest Dnmbp influences Rab11 binding to negative regulators of endosome maturation or inhibits the translocation of Rab11, both of which could lead to accumulation of late endosomes and autophagosomes. Additionally, when combining all the data from this study with the aforementioned studies of the past, we can develop a model in which Dnmbp functions as a critical regulator of epithelial tissue morphogenesis and provides a link between the dynamic processes of actin cytoskeleton regulation, intracellular adhesion, and vesicular transport.

5.2 Future directions

The molecular mechanism of complex processes such as cellular adhesion and vesicular transport, and they affect kidney development, are poorly understood. Recently Dnmbp was implicated in the regulation of dynamic junctions in at least three different ways: (1) through activation of Cdc42 to control junctional configuration (2) by activating N-WASP to promote actin filament branching (3) through direct binding interactions with the Marvel family transmembrane protein known as tricellulin to

facilitate junctional tension. However, these observations were all made within cultured epithelial cell lines. It will be of great interest for future studies to investigate the regulation of these dynamic processes within the developing kidney to gain a better understanding of how cell contacts assemble to form nephric tubules and influence cell signaling to facilitate kidney development. Specifically, investigations into how regulation of vesicular transport and actin regulatory proteins by Dnmbp fits in with adhesion between nephron progenitor cells to enable nephrogenesis. These studies will not only provide us with pivotal knowledge required for understanding how the kidney develops, but also illuminate potential means to cure the abnormalities that arise when that development goes astray.

Chapter 6. Bibliography

1. Kriz, W., & Kaissling, B. (2013). Structural organization of the mammalian kidney. In R. J. Alpern, O. W. Moe, & M. Caplan (Eds.), *Seldin and Giebisch's The Kidney* (5th ed., pp. 595–691). Academic Press.
2. Akilesh, S. (2014). Normal kidney function and structure. In *Pathobiology of human disease* (pp. 2716–2733). Elsevier Inc. <https://doi.org/10.1016/B978-0-12-386456-7.05402-2>
3. Janjua, H. S., Lam, S. K., Gupta, V., & Krishna, S. (2019). Congenital anomalies of the kidneys, collecting system, bladder, and urethra. *Pediatrics in Review*, 40(12), 619–626. <https://doi.org/10.1542/pir.2018-0242>
4. Murugapoopathy, V., & Gupta, I. R. (2020). A primer on congenital anomalies of the kidneys and urinary tracts (CAKUT). *Clinical Journal of the American Society of Nephrology*, 15(5), 723-731. <https://doi.org/10.2215/CJN.12581019>
5. Norman P. Curthoys, N. P., & Moe, O. W. (2014). Proximal tubule function and response to acidosis. *Clinical Journal of the American Society of Nephrology*, 9(9), 1627-1638. <https://doi.org/10.2215/CJN.10391012>
6. Campbell, N. A., Reece, J. B., Urry, L. A., Jackson, R. B., Minorsky, P. V., Wasserman, S. A., & Cain, M. L. (2011). Osmoregulation and excretion. In *Campbell biology* (9th ed., pp. 953–973). Benjamin Cummings.
7. Krieger, P. A. (2009). Urinary System. In *A visual analogy guide to human anatomy & physiology* (pp. 417–444). Morton Publishing.
8. Costantini, F., & Kopan, R. (2010). Patterning a complex organ: Branching morphogenesis and nephron segmentation in kidney development.

Developmental Cell, 18(5), 698–712.

<https://doi.org/10.1016/j.devcel.2010.04.008>

9. Takasato, M., & Little, M. H. (2015). The origin of the mammalian kidney: Implications for recreating the kidney in vitro. *Development*, 142(11), 1937-1947. <https://doi.org/10.1242/dev.104802>
10. Pietilä, I., & Vainio, S. J. (2014). Kidney development: An overview. *Nephron. Experimental Nephrology*, 126(2), 40. <https://doi.org/10.1159/000360659>
11. Little, M. H., & McMahon, A. P. (2012). Mammalian kidney development: Principles, progress, and projections. *Cold Spring Harbor Perspectives in Biology*, 4(5), a008300. <https://doi.org/10.1101/cshperspect.a008300>
12. Blackburn, A. T. M., & Miller, R. K. (2019). Modeling congenital kidney diseases in *Xenopus laevis*. *Disease Models & Mechanisms*, 12(4), dmm038604. <https://doi.org/10.1242/dmm.038604>
13. Corkins, M. E., Achieng, M., DeLay, B. D., Krneta-Stankic, V., Cain, M. P., Walker, B. L., Chen, J., Lindström, N. O., Miller, R. K. (2022). A comparative study of cellular diversity between the *Xenopus* pronephric and mouse metanephric nephron. *bioRxiv*. <https://doi.org/10.1101/2022.01.11.475739>
14. Brändli, A. W. (1999). Towards a molecular anatomy of the *Xenopus* pronephric kidney. *The International Journal of Developmental Biology*, 43(5), 381–395.
15. Hensey, C., Dolan, V., & Brady, H. R. (2002). The *Xenopus* pronephros as a model system for the study of kidney development and pathophysiology. *Nephrology Dialysis Transplantation*, 17(9), 73-74. https://doi.org/10.1093/ndt/17.suppl_9.73

16. Carroll, T., Wallingford, J., Seufert, D., & Vize, P. D. (1999). Molecular regulation of pronephric development. In *Current topics in developmental biology*, 44, (pp. 67–100). [https://doi.org/10.1016/s0070-2153\(08\)60467-6](https://doi.org/10.1016/s0070-2153(08)60467-6)
17. Vize, P. D., Carroll, T. J., & Wallingford, J. B. (2003). Induction, development and physiology of the pronephric tubules, in the kidney. In P. D. Vize, A. S. Woolf, & J. Bard, (Eds.), *Normal development to congenital disease*. Academic Press.
18. Dressler, G. R. (2006). The cellular basis of kidney development. *Annual Review of Cell and Developmental Biology*, 22, 509-529. <https://doi.org/10.1146/annurev.cellbio.22.010305.104340>
19. Bauer, D. V., Huang, S., & Moody, S. A. (1994). The cleavage stage origin of Spemann's Organizer: Analysis of the movements of blastomere clones before and during gastrulation in *Xenopus*. *Development*, 120 (5), 1179–1189. <https://doi.org/10.1242/dev.120.5.1179>
20. Moody, S. A. (1987a). Fates of the blastomeres of the 16-cell stage *Xenopus* embryo. *Development Biology*, 119(2), 560-578. [https://doi.org/10.1016/0012-1606\(87\)90059-5](https://doi.org/10.1016/0012-1606(87)90059-5)
21. Moody, S. A. (1987b). Fates of the blastomeres of the 32-cell-stage *Xenopus* embryo. *Developmental Biology*, 122(2), 300-319. [https://doi.org/10.1016/0012-1606\(87\)90296-x](https://doi.org/10.1016/0012-1606(87)90296-x)
22. DeLay, B. D., Krneta-Stankic, V., & Miller, R. K. (2016). Technique to target microinjection to the developing *Xenopus* kidney. *JoVE*, (111), 53799. <https://doi.org/10.3791/53799>

23. Vize, P. D., Jones, E. A., & Pfister, R. (1995). Development of the *Xenopus* pronephric system. *Developmental Biology*, 171(2), 531-540.
<https://doi.org/10.1006/dbio.1995.1302>
24. Zhou, X., & Vize, P. D. (2004). Proximo-distal specialization of epithelial transport processes within the *Xenopus* pronephric kidney tubules. *Developmental Biology*, 271(2), 322-338.
<https://doi.org/10.1016/j.ydbio.2004.03.036>
25. Sive, H. L., Grainger, R. M., & Harland, R. M. (2000). *Early development of Xenopus laevis: A laboratory manual*. Cold Spring Harbor Laboratory Press.
26. Getwan, M., & Lienkamp, S. S. (2017). Toolbox in a tadpole: *Xenopus* for kidney research. *Cell and Tissue Research*, 369, 143–157.
<https://doi.org/10.1007/s00441-017-2611-2>
27. Jones, E. A. (2005). *Xenopus*: A prince among models for pronephric kidney development. *Journal of the American Society of Nephrology*, 16(2), 313-321.
<https://doi.org/10.1681/ASN.2004070617>
28. Vize, P. D., Seufert, D. W., Carroll, T. J., & Wallingford, J. B. (1997). Model systems for the study of kidney development: Use of the pronephros in the analysis of organ induction and patterning. *Development Biology*, 118(2), 189-204. <https://doi.org/10.1006/dbio.1997.8629>
29. Miller, R. K., Lee, M., & McCrea, P. D. (2014). The *Xenopus* pronephros: A kidney model making leaps toward understanding tubule development. In M. Kloc, J. Z. Kubiak (Eds.), *Xenopus Development* (pp. 215-238). John Wiley & Sons

30. Horster, M. F., Braun, G. S., & Huber, S. M. (1999). Embryonic renal epithelia: Induction, nephrogenesis, and cell differentiation. *Physiological Reviews*, 79(4), 1157–1191. <https://doi.org/10.1152/physrev.1999.79.4.1157>
31. Brennan, H. C., Nijjar, S., & Jones, E. A. (1998). The specification of the pronephric tubules and duct in *Xenopus laevis*. *Mechanisms of Development*, 75(1-2), 127–137. [https://doi.org/10.1016/s0925-4773\(98\)00094-x](https://doi.org/10.1016/s0925-4773(98)00094-x)
32. Carroll, T. J., & Vize, P. D. (1999). Synergism between Pax-8 and lim-1 in embryonic kidney development. *Developmental Biology*, 214(1), 46–59. <https://doi.org/10.1006/dbio.1999.9414>
33. Buisson, I., Le Bouffant, R., Futel, M., Riou, J. F., & Umbhauer, M. (2015). Pax8 and Pax2 are specifically required at different steps of *Xenopus* pronephros development. *Developmental Biology*, 397(2), 175–190. <https://doi.org/10.1016/j.ydbio.2014.10.022>
34. Bracken, C. M., Mizeracka, K., & McLaughlin, K. A. (2008). Patterning the embryonic kidney: BMP signaling mediates the differentiation of the pronephric tubules and duct in *Xenopus laevis*. *Developmental Dynamics: An Official Publication of the American Association of Anatomists*, 237(1), 132–144. <https://doi.org/10.1002/dvdy.21387>
35. Urban, A. E., Zhou, X., Ungos, J. M., Raible, D. W., Altmann, C. R., & Vize, P. D. (2006). FGF is essential for both condensation and mesenchymal-epithelial transition stages of pronephric kidney tubule development. *Developmental Biology*, 297(1), 103–117. <https://doi.org/10.1016/j.ydbio.2006.04.469>

36. Saulnier, D. M., Ghanbari, H., & Brändli, A. W. (2002). Essential function of Wnt-4 for tubulogenesis in the *Xenopus* pronephric kidney. *Developmental Biology*, 248(1), 13–28. <https://doi.org/10.1006/dbio.2002.0712>
37. Carroll, T. J., Wallingford, J. B., & Vize, P. D. (1999). Dynamic patterns of gene expression in the developing pronephros of *Xenopus laevis*. *Developmental Genetics*, 24(3-4), 199–207. [https://doi.org/10.1002/\(SICI\)1520-6408\(1999\)24:3/4<199::AID-DVG3>3.0.CO;2-D](https://doi.org/10.1002/(SICI)1520-6408(1999)24:3/4<199::AID-DVG3>3.0.CO;2-D)
38. Cirio, M. C., Hui, Z., Haldin, C. E., Cosentino, C. C., Stuckenholz, C., Chen, X., Hong, S. K., Dawid, I. B., & Hukriede, N. A. (2011). Lhx1 is required for specification of the renal progenitor cell field. *PLoS One*, 6(4), e18858. <https://doi.org/10.1371/journal.pone.0018858>
39. Jones, E. A. (2003). Molecular control of pronephric development: An overview. *In The Kidney: From Normal Development to Congenital Disease*. (pp. 93–118). Elsevier Inc.
40. Buckley, C. E., & St Johnston, D. (2022). Apical–basal polarity and the control of epithelial form and function. *Nature Reviews Molecular Cell Biology*. <https://doi.org/10.1038/s41580-022-00465-y>
41. Papakrivopoulou, E., Jafree, D. J., Dean, C. H., & Long, D. A. (2021). The biological significance and implications of planar cell polarity for nephrology. *Frontiers in Physiology*, 12, 599529. <https://doi.org/10.3389/fphys.2021.599529>

42. Campanale, J. P., Sun, T. Y., & Montell, D. J. (2017). Development and dynamics of cell polarity at a glance. *Journal of Cell Science*, 130(7), 1201–1207. <https://doi.org/10.1242/jcs.188599>
43. McCaffrey, L. M., Montalbano, J., Mihai, C., & Macara, I. G. (2012). Loss of the Par3 polarity protein promotes breast tumorigenesis and metastasis. *Cancer Cell*, 22(5), 601–614. <https://doi.org/10.1016/j.ccr.2012.10.003>
44. Martin-Belmonte, F., Gassama, A., Datta, A., Yu, W., Rescher, U., Gerke, V., & Mostov, K. E. (2007). PTEN-mediated apical segregation of phosphoinositides controls epithelial morphogenesis through Cdc42. *Cell*, 128:383-397. <https://doi.org/10.1016/j.cell.2006.11.051>
45. Bryant, D. M., Datta, A., Rodríguez-Fraticelli, A. E., Peränen, J., Martín-Belmonte, F., & Mostov, K. E. (2010). A molecular network for de novo generation of the apical surface and lumen. *Nature Cell Biology*, 12(11), 1035–1045. <https://doi.org/10.1038/ncb2106>
46. Cestra, G., Kwiatkowski, A., Salazar, M., Gertler, F., & De Camilli, P. (2005). Tuba, a GEF for CDC42, links dynamin to actin regulatory proteins. *Methods in Enzymology*, 404, 537–545. [https://doi.org/10.1016/S0076-6879\(05\)04047-4](https://doi.org/10.1016/S0076-6879(05)04047-4)
47. Jones, C., & Chen, P. (2007). Planar cell polarity signaling in vertebrates. *BioEssays: News and Reviews in Molecular, Cellular and Developmental Biology*, 29(2), 120–132. <https://doi.org/10.1002/bies.20526>

48. Goodrich, L. V., & Strutt, D. (2011). Principles of planar polarity in animal development. *Development*, 138(10), 1877–1892.
<https://doi.org/10.1242/dev.054080>
49. Oda, Y., Otani, T., Ikenouchi, J., & Furuse, M. (2014). Tricellulin regulates junctional tension of epithelial cells at tricellular contacts through Cdc42. *Journal of cell science*, 127(Pt 19), 4201–4212.
<https://doi.org/10.1242/jcs.150607>
50. Usui, T., Shima, Y., Shimada, Y., Hirano, S., Burgess, R. W., Schwarz, T. L., Takeichi, M., & Uemura, T. (1999). Flamingo, a seven-pass transmembrane cadherin, regulates planar cell polarity under the control of Frizzled. *Cell*, 98(5), 585–595. [https://doi.org/10.1016/s0092-8674\(00\)80046-x](https://doi.org/10.1016/s0092-8674(00)80046-x)
51. Vinson, C. R., Conover, S., & Adler, P. N. (1989). A Drosophila tissue polarity locus encodes a protein containing seven potential transmembrane domains. *Nature*, 338, 263–264. <https://doi.org/10.1038/338263a0>
52. Vinson, C. R., & Adler, P. N. (1987). Directional non-cell autonomy and the transmission of polarity information by the frizzled gene of Drosophila. *Nature*, 329, 549–551. <https://doi.org/10.1038/329549a0>
53. Lu, B., Usui, T., Uemura, T., Jan, L., & Jan, Y. N. (1999). Flamingo controls the planar polarity of sensory bristles and asymmetric division of sensory organ precursors in Drosophila. *Current Biology*, 9(21), 1247–1250.
[https://doi.org/10.1016/s0960-9822\(99\)80505-3](https://doi.org/10.1016/s0960-9822(99)80505-3)

54. Wolff, T., & Rubin, G. M. (1998). Strabismus, a novel gene that regulates tissue polarity and cell fate decisions in *Drosophila*. *Development*, 125(6), 1149–1159. <https://doi.org/10.1242/dev.125.6.1149>
55. Gubb, D., Green, C., Huen, D., Coulson, D., Johnson, G., Tree, D., Collier, S., & Roote, J. (1999). The balance between isoforms of the prickle LIM domain protein is critical for planar polarity in *Drosophila* imaginal discs. *Genes & Development*, 13(17), 2315–2327. <https://doi.org/10.1101/gad.13.17.2315>
56. Krasnow, R. E., Wong, L. L., & Adler, P. N. (1995). Dishevelled is a component of the frizzled signaling pathway in *Drosophila*. *Development*, 121(12), 4095–4102. <https://doi.org/10.1242/dev.121.12.4095>
57. Feiguin, F., Hannus, M., Mlodzik, M., & Eaton, S. (2001). The ankyrin repeat protein Diego mediates frizzled-dependent planar polarization. *Developmental Cell*, 1(1), 93–101. [https://doi.org/10.1016/s1534-5807\(01\)00010-7](https://doi.org/10.1016/s1534-5807(01)00010-7)
58. Butler, M. T., & Wallingford, J. B. (2017). Planar cell polarity in development and disease. *Nature Reviews Molecular Cell Biology*, 18(6), 375–388. <https://doi.org/10.1038/nrm.2017.11>
59. Karner, C. M., Chirumamilla, R., Aoki, S., Igarashi, P., Wallingford, J. B., & Carroll, T. J. (2009). Wnt9b signaling regulates planar cell polarity and kidney tubule morphogenesis. *Nature Genetics*, 41(7), 793–799. <https://doi.org/10.1038/ng.400>
60. Lienkamp, S. S., Liu, K., Karner, C. M., Carroll, T. J., Ronneberger, O., Wallingford, J. B., & Walz, G. (2012). Vertebrate kidney tubules elongate using a planar cell polarity-dependent, rosette-based mechanism of

- convergent extension. *Nature Genetics*, 44(12), 1382–1387.
<https://doi.org/10.1038/ng.2452>
61. Heuzé, M. L., Sankara Narayana, G., D'Alessandro, J., Cellerin, V., Dang, T., Williams, D. S., Van Hest, J. C., Marcq, P., Mège, R. M., & Ladoux, B. (2019). Myosin II isoforms play distinct roles in adherens junction biogenesis. *eLife*, 8, e46599. <https://doi.org/10.7554/eLife.46599>
62. Smutny, M., Cox, H. L., Leerberg, J. M., Kovacs, E. M., Conti, M. A., Ferguson, C., Hamilton, N. A., Parton, R. G., Adelstein, R. S., & Yap, A. S. (2010). Myosin II isoforms identify distinct functional modules that support integrity of the epithelial zonula adherens. *Nature Cell Biology*, 12(7), 696–702.
<https://doi.org/10.1038/ncb2072>
63. Krendel, M. F., & Bonder, E. M. (1999). Analysis of actin filament bundle dynamics during contact formation in live epithelial cells. *Cell Motility and the Cytoskeleton*, 43(4), 296–309. [https://doi.org/10.1002/\(SICI\)1097-0169\(1999\)43:4<296::AID-CM3>3.0.CO;2-U](https://doi.org/10.1002/(SICI)1097-0169(1999)43:4<296::AID-CM3>3.0.CO;2-U)
64. Mège, R. M., & Ishiyama, N. (2017). Integration of cadherin adhesion and cytoskeleton at adherens junctions. *Cold Spring Harbor Perspectives in Biology*, 9(5), a028738. <https://doi.org/10.1101/cshperspect.a028738>
65. Yamada, S., & Nelson, W. J. (2007). Localized zones of Rho and Rac activities drive initiation and expansion of epithelial cell-cell adhesion. *The Journal of Cell Biology*, 178(3), 517–527. <https://doi.org/10.1083/jcb.200701058>
66. Adams, C. L., Chen, Y. T., Smith, S. J., & Nelson, W. J. (1998). Mechanisms of epithelial cell-cell adhesion and cell compaction revealed by high-resolution

- tracking of E-cadherin-green fluorescent protein. *The Journal of Cell Biology*, 142(4), 1105–1119. <https://doi.org/10.1083/jcb.142.4.1105>
67. Strachan, & Read, A. P. (2019). Cell Adhesion and Tissue Formation. In *Human Molecular Genetics* (5th ed, pp. 83-88). CRC Press.
68. Capaldo, C. T., & Macara, I. G. (2007). Depletion of E-cadherin disrupts establishment but not maintenance of cell junctions in Madin-Darby canine kidney epithelial cells. *Molecular Biology of the Cell*, 18(1), 189–200. <https://doi.org/10.1091/mbc.e06-05-0471>
69. Yap, A. S., & Kovacs, E. M. (2003). Direct cadherin-activated cell signaling: A view from the plasma membrane. *The Journal of Cell Biology*, 160(1), 11–16. <https://doi.org/10.1083/jcb.200208156>
70. Coopman, P., & Djiane, A. (2016). Adherens junction and E-Cadherin complex regulation by epithelial polarity. *Cellular and Molecular Life Sciences*, 73(18), 3535–3553. <https://doi.org/10.1007/s00018-016-2260-8>
71. Takeichi, M. (2014). Dynamic contacts: Rearranging adherens junctions to drive epithelial remodelling. *Nature Reviews Molecular Cell Biology*, 15, 397–410. <https://doi.org/10.1038/nrm3802>
72. Pricam, C., Humbert, F., Perrelet, A., & Orci, L. (1974). A freeze-etch study of the tight junctions of the rat kidney tubules. *Laboratory Investigation; A Journal of Technical Methods and Pathology*, 30(3), 286–291.
73. Yu, A., Hanner, F. & Peti-Peterdi, J. (2013). Intercellular Junctions. In R. J. Alpern, O. W. Moe, & M. Caplan (Eds.), *Seldin and Giebisch's The Kidney* (5th ed., pp. 347–368). Academic Press.

74. Hurd, T. W., Gao, L., Roh, M. H., Macara, I. G., & Margolis, B. (2003). Direct interaction of two polarity complexes implicated in epithelial tight junction assembly. *Nature Cell Biology*, 5(2), 137–142. <https://doi.org/10.1038/ncb923>
75. Izumi, Y., & Furuse, M. (2014). Molecular organization and function of invertebrate occluding junctions. *Seminars in Cell & Developmental Biology*, 36, 186–193. <https://doi.org/10.1016/j.semcdb.2014.09.009>
76. Nieuwkoop, P. D., & Faber, J. (1994). *Normal table of Xenopus laevis (Daudin): A systematical & chronological survey of the development from the fertilized egg till the end of metamorphosis*. Garland Publishing
77. Brüser, L., & Bogdan, S. (2017). Adherens junctions on the move-membrane trafficking of E-cadherin. *Cold Spring Harbor Perspectives in Biology*, 9(3), a029140. <https://doi.org/10.1101/cshperspect.a029140>
78. Otani, T., Ichii, T., Aono, S., & Takeichi, M. (2006). Cdc42 GEF Tuba regulates the junctional configuration of simple epithelial cells. *The Journal of cell biology*, 175(1), 135–146. <https://doi.org/10.1083/jcb.200605012>
79. Nanes, B. A., Chiasson-MacKenzie, C., Lowery, A. M., Ishiyama, N., Faundez, V., Ikura, M., Vincent, P. A., & Kowalczyk, A. P. (2012). p120-catenin binding masks an endocytic signal conserved in classical cadherins. *The Journal of Cell Biology*, 199(2), 365–380. <https://doi.org/10.1083/jcb.201205029>
80. Baek, J. I., Kwon, S. H., Zuo, X., Choi, S. Y., Kim, S. H., & Lipschutz, J. H. (2016). Dynamin binding protein (Tuba) deficiency inhibits ciliogenesis and nephrogenesis in vitro and in vivo. *The Journal of Biological Chemistry*, 291(16), 8632–8643. <https://doi.org/10.1074/jbc.M115.688663>

81. Choi, S. Y., Chacon-Heszele, M. F., Huang, L., McKenna, S., Wilson, F. P., Zuo, X., & Lipschutz, J. H. (2013). Cdc42 deficiency causes ciliary abnormalities and cystic kidneys. *Journal of the American Society of Nephrology*, *24*(9), 1435–1450. <https://doi.org/10.1681/ASN.2012121236>
82. Overgaard, C. E., Sanzone, K. M., Spiczka, K. S., Sheff, D. R., Sandra, A., & Yeaman, C. (2009). Deciliation is associated with dramatic remodeling of epithelial cell junctions and surface domains. *Molecular biology of the cell*, *20*(1), 102–113. <https://doi.org/10.1091/mbc.e08-07-0741>
83. Seixas, C., Choi, S. Y., Polgar, N., Umberger, N. L., East, M. P., Zuo, X., Moreiras, H., Ghossoub, R., Benmerah, A., Kahn, R. A., Fogelgren, B., Caspary, T., Lipschutz, J. H., & Barral, D. C. (2016). Arl13b and the exocyst interact synergistically in ciliogenesis. *Molecular Biology of the Cell*, *27*(2), 308–320. <https://doi.org/10.1091/mbc.E15-02-0061>
84. Zuo, X., Fogelgren, B., & Lipschutz, J. H. (2011). The small GTPase Cdc42 is necessary for primary ciliogenesis in renal tubular epithelial cells. *The Journal of Biological Chemistry*, *286*(25), 22469–22477. <https://doi.org/10.1074/jbc.M111.238469>
85. Zuo, X., Lobo, G., Fulmer, D., Guo, L., Dang, Y., Su, Y., Ilatovskaya, D. V., Nihalani, D., Rohrer, B., Body, S. C., Norris, R. A., & Lipschutz, J. H. (2019). The exocyst acting through the primary cilium is necessary for renal ciliogenesis, cystogenesis, and tubulogenesis. *The Journal of Biological Chemistry*, *294*(17), 6710–6718. <https://doi.org/10.1074/jbc.RA118.006527>

86. Blankenship, J. T., Fuller, M. T., & Zallen, J. A. (2007). The *Drosophila* homolog of the Exo84 exocyst subunit promotes apical epithelial identity. *Journal of Cell Science*, 120(Pt 17), 3099–3110. <https://doi.org/10.1242/jcs.004770>
87. Classen, A. K., Anderson, K. I., Marois, E., & Eaton, S. (2005). Hexagonal packing of *Drosophila* wing epithelial cells by the planar cell polarity pathway. *Developmental Cell*, 9(6), 805–817. <https://doi.org/10.1016/j.devcel.2005.10.016>
88. Desclozeaux, M., Venturato, J., Wylie, F. G., Kay, J. G., Joseph, S. R., Le, H. T., & Stow, J. L. (2008). Active Rab11 and functional recycling endosome are required for E-cadherin trafficking and lumen formation during epithelial morphogenesis. *American Journal of Physiology; Cell Physiology*, 295(2), C545–C556. <https://doi.org/10.1152/ajpcell.00097.2008>
89. Langevin, J., Morgan, M. J., Sibarita, J. B., Aresta, S., Murthy, M., Schwarz, T., Camonis, J., & Bellaïche, Y. (2005). *Drosophila* exocyst components Sec5, Sec6, and Sec15 regulate DE-Cadherin trafficking from recycling endosomes to the plasma membrane. *Developmental Cell*, 9(3), 365–376. <https://doi.org/10.1016/j.devcel.2005.07.013>
90. Woichansky, I., Beretta, C. A., Berns, N., & Riechmann, V. (2016). Three mechanisms control E-cadherin localization to the zonula adherens. *Nature Communications*, 7, 10834. <https://doi.org/10.1038/ncomms10834>
91. Yeaman, C., Grindstaff, K. K., & Nelson, W. J. (2004). Mechanism of recruiting Sec6/8 (exocyst) complex to the apical junctional complex during polarization

- of epithelial cells. *Journal of Cell Science*, 117(Pt 4), 559–570.
<https://doi.org/10.1242/jcs.00893>
92. Wu, S., Mehta, S. Q., Pichaud, F., Bellen, H. J., & Quioco, F. A. (2005). Sec15 interacts with Rab11 via a novel domain and affects Rab11 localization in vivo. *Nature Structural & Molecular Biology*, 12(10), 879–885.
<https://doi.org/10.1038/nsmb987>
93. Zhang, X. M., Ellis, S., Sriratana, A., Mitchell, C. A., & Rowe, T. (2004). Sec15 is an effector for the Rab11 GTPase in mammalian cells. *The Journal of Biological Chemistry*, 279(41), 43027–43034.
<https://doi.org/10.1074/jbc.M402264200>
94. Giansanti, M. G., Belloni, G., & Gatti, M. (2007). Rab11 is required for membrane trafficking and actomyosin ring constriction in meiotic cytokinesis of *Drosophila* males. *Molecular Biology of the Cell*, 18(12), 5034–5047.
<https://doi.org/10.1091/mbc.e07-05-0415>
95. Qin, Y., Meisen, W. H., Hao, Y., & Macara, I. G. (2010). Tuba, a Cdc42 GEF, is required for polarized spindle orientation during epithelial cyst formation. *The Journal of Cell Biology*, 189(4), 661–669.
<https://doi.org/10.1083/jcb.201002097>
96. Ossipova, O., Kim, K., Lake, B. B., Itoh, K., Ioannou, A., & Sokol, S. Y. (2014). Role of Rab11 in planar cell polarity and apical constriction during vertebrate neural tube closure. *Nature Communications*, 5, 3734.
<https://doi.org/10.1038/ncomms4734>

97. DeLay, B. D., Baldwin, T. A., & Miller, R. K. (2019). Dynamin binding protein is required for *Xenopus laevis* kidney development. *Frontiers in Physiology*, 10, 143. <https://doi.org/10.3389/fphys.2019.00143>
98. Salazar, M. A., Kwiatkowski, A. V., Pellegrini, L., Cestra, G., Butler, M. H., Rossman, K. L., Serna, D. M., Sondek, J., Gertler, F. B., & De Camilli, P. (2003). Tuba, a novel protein containing bin/amphiphysin/Rvs and Dbl homology domains, links dynamin to regulation of the actin cytoskeleton. *The Journal of Biological Chemistry*, 278(49), 49031–49043. <https://doi.org/10.1074/jbc.M308104200>
99. Shindo, A., & Wallingford, J. B. (2014). PCP and septins compartmentalize cortical actomyosin to direct collective cell movement. *Science*, 343(6171), 649–652. <https://doi.org/10.1126/science.1243126>
100. Carman, P. J., & Dominguez, R. (2018). BAR domain proteins—a linkage between cellular membranes, signaling pathways, and the actin cytoskeleton. *Biophysical Reviews*, 10(6), 1587–1604. <https://doi.org/10.1007/s12551-018-0467-7>
101. Ossipova, O., Kim, K., Lake, B. B., Itoh, K., Ioannou, A., & Sokol, S. Y. (2014). Role of Rab11 in planar cell polarity and apical constriction during vertebrate neural tube closure. *Nature Communications*, 5, 3734. <https://doi.org/10.1038/ncomms4734>
102. Moody, S. A., & Kline, M. J. (1990). Segregation of fate during cleavage of frog (*Xenopus laevis*) blastomeres. *Anatomy and Embryology*, 182(4), 347–362.

103. Szatmári, Z., Kis, V., Lippai, M., Hegedus, K., Faragó, T., Lorincz, P., Tanaka, T., Juhász, G., & Sass, M. (2014). Rab11 facilitates cross-talk between autophagy and endosomal pathway through regulation of Hook localization. *Molecular Biology of the Cell*, 25(4), 522–531.
104. Bryant, D. M., & Stow, J. L. (2004). The ins and outs of E-cadherin trafficking. *Trends in Cell Biology*, 14(8), 427–434.
105. Krneta-Stankic, V., Corkins, M. E., Paulucci-Holthauzen, A., Kloc, M., Gladden, A. B., & Miller, R. K. (2021). The Wnt/PCP formin Daam1 drives cell-cell adhesion during nephron development. *Cell Reports*, 36(1), 109340. <https://doi.org/10.1016/j.celrep.2021.109340>
106. Kovacs, E. M., Makar, R. S., & Gertler, F. B. (2006). Tuba stimulates intracellular N-WASP-dependent actin assembly. *Journal of Cell Science*, 119(Pt 13), 2715–2726. <https://doi.org/10.1242/jcs.03005>
107. Davidson, L.A., Marsden, M., Keller, R., and DeSimone, D.W. (2006). Integrin $\alpha 5 \beta 1$ and Fibronectin Regulate Polarized Cell Protrusions Required for *Xenopus* Convergence and Extension. *Curr. Biol.* 16, 833–844.
108. Lyons, J.P., Miller, R.K., Zhou, X., Weidinger, G., Deroo, T., Denayer, T., Park, J., Ji, H., Hong, J.Y., Li, A., et al. (2009). Requirement of Wnt/beta catenin signaling in pronephric kidney development. *Mech. Dev.* 126, 142–159.
109. Miller, R.K., Gomez de la Torre Canny, S., Jang, C.-W., Cho, K., Ji, H., Wagner, D.S., Jones, E.A., Habas, R., and McCrea, P.D. (2011). Pronephric Tubulogenesis Requires Daam1-Mediated Planar Cell Polarity Signaling. *J. Am. Soc. Nephrol.* 22, 1654–1664.

Vita

Brandy Lynn Walker completed her Associate of Science in Biology in 2016 at Lone Star College in The Woodlands, TX. She graduated from University of Houston-Downtown with a Bachelor of Science with a Concentration in Microbiology in December 2019. In January of 2020, she entered The University of Texas MD Anderson Cancer Center UTHealth Graduate School of Biomedical Sciences.